COSMOS-Europe: A European Network of Cosmic-Ray Neutron Soil Moisture Sensors

Heye R. Bogena[1,*], Martin Schrön[2]~~,~~[,*], Jannis Jakobi[1], Patrizia Ney[1], Steffen Zacharias[2], Mie Andreasen[3], Roland Baatz[1], David Boorman[4], Berk M. Duygu[5], Miguel A. Eguibar-Galán[6], Benjamin Fersch[7], Till Franke[8], Josie Geris[9], María González Sanchis[10], Yann Kerr[11], Tobias Korf[1], Zalalem Mengistu[12], Arnaud Mialon[11], Paolo Nasta[13], Jerzy Nitychoruk[14], Vassilios Pisinaras[15], Daniel Rasche[16], Rafael Rosolem[17], Hami Said[18], Paul Schattan[19], Marek Zreda[20], Stefan Achleitner[19], Eduardo Albentosa-Hernández[6], Zuhal Akyürek[5], Theresa Blume[16], Antonio del Campo[10], Davide Canone[24], Katya Dimitrova-Petrova[9], John G. Evans[4], Stefano Ferraris[24], Félix Frances[6], Davide Gisolo[24], Andreas Güntner[16], Frank Herrmann[1], Joost ~~Iwema[17]~~Iwema[25], Karsten H. Jensen[21], Harald Kunstmann[7, 22], Antonio Lidón[10], Majken C. Looms[21], Sascha Oswald[8], Andreas Panagopoulos[15], Amol Patil[22], Daniel Power[17], Corinna Rebmann[2], Nunzio Romano[13], Lena M. Scheiffele[8], Sonia Seneviratne[23], Georg Weltin[18] and Harry Vereecken[1]

[1] Agrosphere Institute (IBG-3), Forschungszentrum Jülich GmbH, 52425 Jülich, Germany.
[2] Helmholtz Centre for Environmental Research GmbH, 04318 Leipzig, Germany
[3] Geological Survey of Denmark and Greenland, 1350 Copenhagen, Denmark
[4] UK Centre for Ecology & Hydrology, Wallingford, OX10 8BB, UK
[5] Water Resources Laboratory of Civil Engineering Department, Middle East Technical University, 06800 Ankara, Turkey
[6] Research Institute of Water and Environmental Engineering (IIAMA), Universitat Politècnica de València, 46022 Valencia, Spain
[7] Karlsruhe Institute of Technology, Campus Alpine (IMK-IFU), 82467 Garmisch-Partenkirchen, Germany
[8] Institute of Environmental Science and Geography, University of Potsdam, 14476 Potsdam, Germany
[9] Northern Rivers Institute, School of Geosciences, University of Aberdeen, Aberdeen, UK
[10] Hydraulic and environmental Engineering Department, Universitat Politècnica de València, 46022 Valencia, Spain
[11] CESBIO Université Toulouse 3 (CNES, CNRS, INRAE, IRD, UPS), 31401 Toulouse, France
[12] Norwegian water resources and energy directorate, 0301 Oslo, Norway
[13] Dep. of Agricultural Sciences, AFBE Division, University of Napoli Federico II, Portici (Napoli), Italy
[14] Pope John Paul II State School of Higher Education, 95/97, Biala Podlaska, Poland
[15] Soil & Water Resources Institute, Hellenic Agricultural Organization "DEMETER", 57400 Sindos (Thessaloniki), Greece
[16] GFZ German Research Centre for Geosciences, Section Hydrology, 14473 Potsdam, Germany
[17] Department of Civil Engineering, University of Bristol, BS8 1TH Bristol, UK
[18] Soil and Water Management & Crop Nutrition Laboratory, Joint FAO/IAEA Centre of Nuclear Techniques in Food and Agriculture, Department of Nuclear Sciences and Applications, International Atomic Energy Agency, Vienna, Austria
[19] University of Innsbruck, Innsbruck, Austria
[20] Dep. of Hydrology and Atmospheric Sciences, University of Arizona, Tucson, USA
[21] Department of Geosciences and Natural Resource Management, University of Copenhagen, Copenhagen, Denmark
[22] Institute of Geography, University of Augsburg, 86159 Augsburg, Germany
[23] Dep. of Environmental Systems Science, ETH Zürich, CHN N 11, 8092 Zürich, Switzerland

[24] Dep. of Regional and Urban Planning, Politecnico and University of Turin, 10125 Turin, Italy
[25] Wageningen University & Research, Wageningen, The Netherlands
* these authors contributed equally to this manuscript

Correspondence to: Heye R. Bogena (h.bogena@fz-juelich.de)

Abstract. ~~Human-caused climate~~Climate change increases the occurrence and severity of droughts due to increasing temperatures, altered circulation patterns and reduced snow occurrence. ~~For example,~~While Europe has suffered from drought events in the last decade ~~like never~~unlike ever seen since the beginning of weather ~~recording.~~recordings, harmonized long-term datasets across the continent are needed to monitor change and support predictions. Here we present soil moisture data from ~~65 Cosmic~~66 cosmic-ray neutron sensors (CRNS) in Europe (COSMOS-Europe for short) covering recent drought events. The CRNS sites are distributed across Europe and cover all major land use types and climate zones in Europe. The raw neutron count data from the CRNS stations were provided by ~~23~~24 research institutions and processed using state-of-the-art

Formatiert: Schriftfarbe: Automatisch

Formatiert: Schriftfarbe: Automatisch

methods. The harmonised processing included correction of the raw neutron counts, and a harmonised methodology for the conversion into soil moisture based on available in-situ information. In addition, ~~information on~~ the ~~data~~ uncertainty estimate is provided with the dataset, information that is particularly useful for remote sensing and modelling applications. This paper presents the current spatiotemporal coverage of CRNS stations in Europe and describes the protocols for data processing from raw measurements to consistent soil moisture products~~ as well as first results on how the recent drought events have been captured by the CRNS network. This harmonised European soil moisture dataset will help both hydrologists and climate scientists to study individual drought events, to understand their causes, to evaluate and improve their modelling, and to estimate the extremity of current events.~~. The data of the presented COSMOS-Europe network open up a manifold of potential applications for environmental research, such as remote sensing data validation, trend analysis, or model assimilation. The data set could be of particular importance for the analysis of extreme climatic events at the continental scale. Due its timely relevance in the scope of climate change in the recent years, we demonstrate this potential application with a brief analysis on the spatiotemporal soil moisture variability. The dataset, entitled “Dataset of COSMOS-Europe: A European network of Cosmic-Ray Neutron Soil Moisture Sensors”, is shared via Forschungszentrum Jülich: https://doi.org/10.34731/x9s3-kr48 (Bogena and Ney, 2021).

1 Introduction

Formatiert: Schriftfarbe: Automatisch

The ~~summers of~~years 2003, 2010, 2015, and 2018 are considered as the most notable years of the 21st century in Europe in terms of summer drought~~ but~~, and also witnessed numerous heat-related deaths (Stott et al., 2004; Ionita et al., 2017; Laaha et al., 2017; Schuldt et al., 2020; Sutanto et al., 2020~~)~~), and extensive forest fires (Fink et al., 2004; Grumm, 2011; Turco et al., 2017~~), which~~). This has stimulated a debate on how changes in the occurrence and characteristics of drought are related to climatic variability (e.g., Hanel et al., 2018; Hisdal et al., 2001; Seneviratne et al., 2012; Sheffield et al., 2012). During the most recent heatwave in 2018, daily temperature anomalies reached up to 14 °C in Scandinavia and Central Europe and impacted the energy and carbon balance of European terrestrial ecosystems (Graf et al., 2020). This heat wave was exacerbated by a drought caused by a persistent circulation anomaly (Kornhuber et al., 2019), which additionally fostered unprecedented wildfires in Europe (e.g., Yiou et al., 2020). Recently, Humphrey et al. (2021) ~~showed~~have shown that soil moisture variability explains 90 % of the interannual variability in global carbon uptake~~, with most of the ecosystem response occurring indirectly as a~~. The corresponding feedback between soil moisture and the atmosphere~~, amplifying~~ amplifies temperature and ~~humidity~~moisture anomalies and ~~exacerbating~~intensifies the direct effects of ~~droughts~~drought and soil water stress. In this respect, ground-based soil moisture measurements are indispensable to better understand the land surface – atmosphere interactions leading to droughts and soil water stress.

Recent advances in measurement techniques, such as cosmic-ray neutron probes, allow continuous non-invasive soil moisture measurements that integrate over scales beyond the traditional point measurement (Zreda et al. 2012; Bogena et al., 2015; Andreasen et al., 2017). In the 1950s it was discovered that neutron scattering could be used as a method of measuring soil moisture (e.g., Gardner and Kirkham, 1952) and this was to become the main means of quantifying water storage in soils for the next three decades. The neutron probe contains a radioactive source that generates fast neutrons that are decelerated by the hydrogen of the soil water to thermal neutrons, so that the detected thermal neutron count rate is closely related to the soil water content. Thanks to the pioneering work of Topp et al. (1980), from the 1980s the electromagnetic measurement technology became established for simple and continuous monitoring of soil moisture dynamics. As a result, neutron probes were hardly used anymore and interest in neutron scattering in soils declined until the introduction of the cosmic-ray neutron measurement method (Zreda et al., 2008) generated renewed interest. Recently, neutron scattering is again considered one of the most promising soil moisture measurement techniques, as cosmic neutron sensors (CRNS) provide non-invasive soil moisture at the field scale with an effective radius of 130 to 240 m and a penetration depth of 15 to 55 cm depending on soil wetness (Köhli et al., 2015; Schrön et al., 2017). In contrast to the classical active neutron probe, the CRNS is placed above ground and detects cosmogenic neutrons. The CRNS can be calibrated by comparing the neutron count rate with gravimetric soil moisture sampling data averaged over the CRNS footprint by a weighting function (Schrön et al., 2017). The CRNS shows excellent data acquisition reliability and can be applied also in vegetated areas ~~prone~~ with low to medium biomass such as cropped fields (Rivera Villarreyes et al., 2011; Franz et al., 2013) and forests (Bogena et al., 2013; Heidbüchel et al., 2016; Vather et al., 2020). During the last decade, several studies applied and progressed the CRNS technique both on stationary and mobile platforms up to the scale of square kilometres (Fersch et al., 2020; Schrön et al., ~~2018a~~2018) and by monitoring stations installed in a broad variety of climate conditions, namely: continental (e.g., Baatz et al., 2014), temperate (e.g., Evans et al., 2016), semi-arid (e.g., Zreda et al., 2012), and tropical (e.g., Hawdon et al., 2014). The advantages of the ~~CNRS~~CRNS technique have promoted its application in various fields, such as hydrology (e.g., Dimitrova-Petrova et al., 2020a; Schattan et al., 2020), snow monitoring (e.g., Bogena et al., 2020; Schattan et al., 2017), precipitation monitoring (Franz et al., 2020~~)~~), vegetation monitoring (e.g., Franz et al., 2013; Jakobi et al., 2018), validation of remote sensing products (e.g., Montzka et al., 2017; Duygu and Akyürek, 2019), land surface modelling (e.g., Shuttleworth et al., 2013; Baatz et al., 2017; Brunetti et al., 2019; Iwema et al., 2017, Patil et al. 2021), and agricultural management (e.g., Finkenbiner et al., 2018; Li et al., 2019).

Formatiert: Schriftart: +Überschriften (Times New Roman)

According to Andreasen et al. (2017a), there are currently ~~about~~more than 200 stationary CRNSs ~~operating~~operated worldwide, often as regional networks in hydrological observatories (e.g., Bogena et al., 2018; Kiese et al., 2018; Lui et al., 2018) or in entire countries (Zreda et al., 2012; Hawdon et al., 2014; Evans et al., 2016). This paper introduces the network of existing CRNS stations in Europe (COSMOS-Europe for short) and how ~~we process~~ the data is processed in a harmonised way. We present the current instrumentation and the protocols developed to process the raw measurements and how the CRNS stations have been recalibrated to derive soil moisture in a more consistent way. Based on the processed CRNS soil moisture time series, we then performed a brief analysis on the spatiotemporal occurrence of drought events in Europe.

2 Overview of the COSMOS-Europe sites

Formatiert: Schriftfarbe: Automatisch

For the COSMOS-Europe dataset presented here, CRNS data from ~~63~~66 sites in 12 European countries (in alphabetical order: Austria, Denmark, France, Germany, Greece, Italy, Norway, Poland, Spain, Switzerland, Turkey, United Kingdom) were collected. The geographical distribution and location of the COSMOS-Europe sites is shown in Fig. 1. ~~A summary description of~~The key environmental and soil-related physical properties at the ~~individual~~ sites is given in Table 1. The key physical and soil-related site properties relevant to CRNS processing are summarized in Table 2.

The COSMOS-Europe sites cover eight climatic zones (following the Köppen-Geiger climate classification (Beck et al., 2018)), with the vast majority of stations located in the humid continental climate zone (n=34) and in the temperate oceanic climate zone (n=21). The remaining ~~12~~ sites are located in six further climate zones. ~~The~~According to site owner information, the majority of COSMOS-Europe sites are managed grassland (n=23) and cropland (n=23), while the remaining sites are covered by forest (n=7), forest clear-cut (n=1), shrubland (n=5), heathland (n=2), orchard/plantation (n=2), bare rock/glacier (n=1), moorland (n=1), and sparse vegetation (n=1).

The soils of the COSMOS-Europe sites range from organic soils with a high organic matter content (max: 0.173 g/g) to mineral soils with very low organic matter content (min: 0.004 g/g). This variability is also reflected in the wide range of soil porosities ranging from 0.365 to 0.841. Two of the sites, Weisssee and Zugspitze, are located in rocky, alpine terrain. The Weisssee data only shows ~~few~~limited and short snow-free periods where soil moisture data is available and with high uncertainties due to the difficult soil sampling in that area. The data from Zugspitze is not used for soil moisture analysis due to the absence of soil, but offers great potential for other hydrological studies, such as snow water equivalent monitoring.

The measurements of neutron count rates and corresponding correction data (i.e. atmospheric pressure and air humidity) at the COSMOS-Europe sites cover very different periods of time (cf. Fig. 2 and Tab. 1). The shortest time series comes from the

Zerbst site, which was put into operation in late 2020. The longest time series from the Wüstebach1 site spans a period of approximately 10 years (mid-2011 to present). The average length of the observation periods of all sites is 5.7 years (±2.78). The geographic distribution of the COSMOS-Europe stations also reflects strong gradients of cutoff rigidities – a quantity describing the shielding of incoming cosmic-ray particles by Earth's geomagnetic field. Therefore, the dynamics and intensity of cosmic rays at stations in northern Europe are significantly higher than at stations further south. The cutoff rigidity ranges from 1.21 GeV for the Aas site in Norway to 8.37 for the Cakit Basin site in Turkey.

More than 50 additional sites are indicated in Fig. 1 (black cross) which are not specifically addressed in this manuscript. They either belong to other networks with dedicated data publications (e.g., COSMOS-UK or the intensive research experiment in Marquardt near Berlin), or were installed just recently (e.g., Prague and Northwest Germany), or refer to planned COSMOS locations in the near future (e.g., Finland and Ireland). There are even more stations across Europe that operate sub-snow cosmic-ray neutron detectors (Gugerli et al~~.~~., 2019). Due to the slightly different measurement technique, the point-scale footprint, and the exclusive focus on snow monitoring, those sensors were not included in this paper and deserve dedicated articles.

3 Methods

Formatiert: Schriftfarbe: Automatisch

~~3.1 Data pre-processing~~

Measured neutrons are a proxy for soil water content, but systematic factors and stochastic effects also influence the neutron signal. Research in the last decades has led to a profound understanding of these influencing factors and has facilitated a more accurate extraction of the soil moisture signal from the cosmic-ray neutron data. The processing framework is described below, while its technical implementation is supported by public tools and software libraries dedicated to CRNS research~~(~~, e.g., Corny~~, https://git.ufz.de/CRNS/cornish_pasdy, or~~ by Schrön (2021a), Crspy by Power et al. (2021).

Formatiert: Schriftart: Nicht Fett

Formatiert: Überschrift 2, Zeilenabstand: 1,5 Zeilen

Formatiert: Schriftart: Nicht Fett

Formatiert: Schriftart: Nicht Fett

Formatiert: Schriftart: Nicht Fett

Formatiert: Englisch (Vereinigtes Königreich)

3.1 Data pre-processing

In a first step, all data sets, i.e. raw neutron counts and supporting data, were aggregated to hourly time steps. Subsequently, following Zreda et al. (2008), a running 24-hour average with a minimum of 12 measurements in the smoothing window was used to reduce the inherent noise of the raw neutron counts and to reduce the measurement uncertainty.

To ensure data consistency, the raw neutron counts were screened for data quality. Suspicious neutron count rates (N_{raw}) that fulfill one of the following conditions were flagged:

- Extreme single outliers: N_{raw}< 50 or N_{raw}> 10000 counts per hour (cph)
- Positive suspicious peaks: N_{raw}> 24h moving average + 2 times the standard deviation of the 24h rolling sum
- Negative suspicious peaks: N_{raw}< 24h moving average - 2 times the standard deviation of the 24h rolling sum

Neutron count rates can be strongly affected by the presence of snow cover, resulting in inaccurate soil moisture measurements. Unfortunately, in most cases no additional snow measurements were available at the CRNS sites. Therefore, we used the ECMWF climate reanalysis data product ERA5~~ (https://www.ecmwf.int/en/research/climate-reanalysis)~~-Land (Muñoz Sabater, 2019) to indicate snow cover events. For this, we flagged neutron count data when the 24-hour moving average of the ERA5 SWE (snow water equivalent) product exceeded 1 mm.

Formatiert: Schriftfarbe: Automatisch

To indicate unrealistically high values in the CRNS-derived soil moisture time series, we flagged values for soil moisture that were greater than local soil porosity. Because local measurements of soil porosity were not available, we estimated porosity using available information on bulk density and soil organic carbon content. We assumed that soil organic matter was two times the organic carbon content and assumed densities of 1.4 and 2.65 g/cm³ for the organic matter and the other soil minerals, respectively. ~~If no information was available~~Missing data on ~~the~~ soil texture, porosity and organic carbon ~~content, a porosity of 0.5 was assumed.~~where taken from the global raster-based soil dataset SoilGrids (Hengl et al. 2017).

It is important to note that the published dataset still includes the original and flagged data, while suspicious records were not included in the further data processing and analysis (see Figure A5 for the used data flags). In this way, users can apply their own pre-processing techniques to the raw neutron count data. The final soil moisture product is cleaned from all negative influences to avoid inexperienced users using unrealistic soil moisture data.

The local air temperature, air humidity, and atmospheric pressure data needed for the correction of raw neutron counts often contained gaps due to measurement failure or due to removing suspicious data using max/min filters (see Figure 2). These data gaps were filled with ERA5 data following the idea of Power et al. (2021). To ensure consistency of the data, linear regression models of the individual data time series were created to scale the ERA5 data to the local data prior to gap filling. Linear regression is necessary to compensate for differences in bias and slope, e.g., because due to the low spatial resolution of ERA5 (~31 km), the average altitude, humidity and atmospheric pressure for the ERA5 grid does not match those at the COSMOS-Europe site. These deviations occur especially in the high mountains due to strong elevation differences, e.g., for atmospheric pressure at the Leutasch site (see Fig. A2). The regression analysis showed that the ERA5 data mostly agreed well with the local measurements (Figs. A1 and A2), with mean correlations between ERA5 and local measurements of 0.95 for atmospheric pressure and 0.86 for absolute humidity. When the correlation coefficients for humidity and atmospheric pressure were less than 0.7 and 0.8, respectively, the local measurements were replaced entirely by ERA5 data to avoid inconsistencies in the gap-filled time series.

Formatiert: Schriftfarbe: Automatisch

Formatiert: Schriftfarbe: Automatisch

3.2 Correction of raw neutron counts

Variations of the incoming cosmic-ray intensity can have many causes, from galactic and solar disturbances to atmospheric and meteorological influences. Most of these anomalies are expected to change proportionally in every domain of the neutron energy spectrum and thus can be addressed by applying a set of correction factors, :

$$N = N_{\text{raw}} \cdot C_p \cdot C_h \cdot C_{\text{inc}} \cdot C_{\text{veg}} \tag{1}$$

The determination of the correction factors is explained in the following.

3.2.1 Atmospheric pressure correction

Since the cosmic-ray flux through the atmosphere is exponentially attenuated as a function of the traversed cumulative mass, measured neutron count rates can be normalized to standard atmospheric pressure by applying the standard pressure correction approach (Desilets and Zreda, 2003):

$$C_p = e^{\beta(p-p_0)} \tag{2}$$

where C_p is atmospheric pressure correction factor, P_0 is the reference atmospheric pressure (1013.25 hPa), P is the actual atmospheric pressure, and β=0.0076 is the barometric coefficient that is related to the local mass attenuation length of neutrons in air. We also tested the application of regionally variable values for β according to Desilets and Zreda (2003, 2006), but found only negligible variations over Europe. However, future work should further investigate the influence of local β variability on the atmospheric pressure correction.

3.2.2 Air humidity correction

We accounted for the effect of atmospheric water vapor fluctuations on neutron count rate using the approach of Rosolem et al. (2013):

$$C_h = 1 + \alpha\, h \tag{3}$$

with α = 0.0054 and *h* is the absolute humidity (g/m³) measured at 2 m height.

3.2.3 Incoming neutron correction

The galactic cosmic radiation, or incoming radiation *I(t)*, that penetrates the upper atmosphere varies in time mainly due to the well-known 11-year cycle of the solar activity. At high solar power (the solar maximum), the stronger solar magnetic field deflects a larger proportion of galactic particles away from Earth and reduces *I(t)*. Conversely, during low solar activity (the solar minimum) the weaker solar magnetic field allows more galactic protons to enter the atmosphere increasing *I(t)*. Shorter-term fluctuations have a similar effect on *I(t)*, but with lower amplitude. Changes in the shape of the geomagnetic field, which occur on time scales from years to decades, are of secondary importance compared to temporal fluctuations of *I(t)*. These temporal variations are measured locally with so-called neutron monitors (NM), which are sensitive to high-energy secondary neutrons (> 20 MeV) but insensitive to local environmental factors (Simpson, 2000). The incoming radiation varies also spatially with strong gradients from the pole to the equator, corresponding to the cutoff rigidity of the Earth's magnetic field. A worldwide network of NM stations provides near real-time access to incoming cosmic-ray data (https://nmdb.eu). Assuming that the incoming radiation along the rigidity lines is similar, a nearby NM should be able to provide representative data for other places on Earth with similar cut-off rigidity R_{cut}. The local R_{cut} can be estimated for individual CRNS stations using approaches provided by Butikofer et al. (2007). Since every detector comes with an individual efficiency, the value *I(t)* could be normalized with an arbitrary but constant reference I_{ref}, which we chose to be 150 cps. However, NM stations are rare, representing only a few latitudes and often not providing continuous signals over long periods of time. The NM at Jungfraujoch (Switzerland) is one of the few stations that provides reliable long-term data that can be used for COSMOS stations in Europe due its central location. Hence, scaling of the Jungfraujoch signal is needed to match the wide-spread distribution of COSMOS stations in Europe. According to Schrön et al. (~~2015~~2016), the intensity correction factor can be calculated as follows:

$$C_{\mathrm{inc}} = \left[1 + \gamma\,(I/I_{\mathrm{ref}} - 1)\right]^{-1} \tag{4}$$

in which *I* is the count rate of incoming cosmic-ray neutrons of a neutron monitoring station, I_{ref} is the incoming count rate at an arbitrary time, and is an amplitude scaling factor to adjust for the mentioned geomagnetic effects. It depends on the cutoff rigidity of the local site and the neutron monitor used (see e.g., Hawdon et al. 2014). For this paper, we use the approach from Hawdon~~,~~ et al. (2014) to bridge the regional difference of cutoff rigidities between the local site and the NM.

3.2.4 Biomass correction

Biomass can affect neutron count rates and should be considered when large temporal changes in biomass occur at a CRNS site. Therefore, we consider the biomass correction method proposed by Baatz et al. (2015) using the dry biomass *B* in kg/m²:

$$C_{\mathrm{veg}} = \left[1 - 0.009248\, B\right]^{-1} \tag{5}$$

This correction was applied at the Wuestebach1 site, where a large change in biomass had occurred in the CRNS footprint area due to clearcutting of a forest. For the other sites, there were no strong biomass changes or no detailed information on biomass changes was available. As soon as changes in the biomass occur or information for a site is available, these can be taken into account.

3.3 Sensor calibration

3.3.1 In-situ reference soil data

For the calibration, we used in most cases available information on gravimetrically measured soil moisture from soil samples taken within the CRNS footprint. The soil samples were weighted vertically according to Schrön et al. (2017), i.e. for each sample at depth *d* and penetration depth *D* we evaluate the weight in the representative sample volume (d_1 to d_2) to generate the profile average soil moisture:

$$\theta_{\text{profile}} = \frac{\sum \theta_d \, w_d}{\sum w_d}\,, \quad \text{where} \quad w_d = \int_{d_1}^{d_2} W_d \, \mathrm{d}d \propto W_{d_1} - W_{d_2} \tag{6}$$

In addition, we applied horizontal weighting of the vertically averaged in-situ soil moisture according to Schrön et al. (2017). For this, regions of equal contribution (annuluses of 20% quantiles) to the neutron signal were defined depending on the local conditions (i.e. atmospheric pressure, air humidity, average soil moisture) that influence the spatial sensitivity of the CRNS. All sampling points that fall within an annulus *A* are arithmetically averaged and thus receive the same weights, which are calculated according to the weighting scheme of Schrön et al. (2017). More specifically, θ_{horiz} is integrated over the entire domain to find the radii r_1 and r_2 that define the five annuluses $A(r_1,r_2)$ within which all samples are equally averaged:

$$\theta_{\text{horiz}} = \frac{1}{5}\sum_{A=1}^{5} \theta_A\,,$$
$$\text{where} \quad \theta_A = \langle \theta_r \rangle \;\; \forall r \in (r_1, r_2) \quad \text{with} \quad \int_{r_1}^{r_2} W_r \, \mathrm{d}r = \frac{A}{5}\int_0^{\infty} W_r \, \mathrm{d}r \tag{7}$$

In particular, this method ensures that soil samples taken using the outdated COSMOS scheme (25, 75, 200 m), which assumed larger CRNS footprints, are not double weighted. Due to the long distances of the COSMOS sampling scheme, there may be no soil samples in one annulus. In this case, the samples in the next larger ring receive double the weight, i.e. the soil samples taken at 25 m distance are also representative for the soil moisture in the first annulus around the sensor. This problem does not arise for COSMOS-Europe sites sampled according to the revised weighting scheme of Schrön et al. (2017), as soil samples were also taken in the near field of the CRNS (i.e., 2-10 m distances). The in-situ reference soil moisture of COSMOS-Europe sites as well as the weighted averages used for the CRNS soil moisture calibration are presented in Figure A4.

3.3.2 Conversion of neutron count rate to soil moisture

To convert neutron count rates to soil moisture, we used the conventional relationship between neutrons and soil moisture initially introduced by Desilets et al. (2010). According to Köhli et al. (2021), it can be expressed in an equivalent but more unambiguous formulation with fewer parameters:

$$\theta(N) = \frac{0.0808}{N/N_0 - 0.372} - 0.115 \quad \equiv \quad p_0\,\frac{1 - N/N_{\text{max}}}{p_1 - N/N_{\text{max}}} \tag{8}$$

where N_{max} is the maximum neutron flux under dry conditions which mainly depends on the individual detector sensitivity. Parameters $p_0 = -0.115$, $p_1 = 0.346$, and $N_{max} = 1.075 * N_0$ can be derived from the parameters used so far in the Desilets equation.

Hydrogen in the organic matter as well as the lattice water content of soils affects how epithermal neutrons interact with the soil, and thus affects the shape of the calibration function (Zreda et al., 2012). We accounted for this effect by fitting N_{max} of the calibration to the total soil water, which is the sum of the water equivalents of lattice water and organic matter and the gravimetrically measured reference soil moisture. The volumetric soil moisture is then obtained by subtracting the lattice and organic matter water from CRNS total soil moisture multiplied with the soil density. We averaged the soil property values, in case multiple calibration dates were available. In order to increase the signal-to-noise ratio of the neutron counts we applied a moving average with a window size of 24 hours for the N_{max} calibration. It should be noted that a 24-hour window is well suited for drought studies, but may mask the signal from wetting events, which tend to occur much faster.

3.4 Soil moisture uncertainty

The statistical uncertainty of CRNS-derived soil moisture scales with the number of counts in a given period. However, this count rate is inversely related to soil moisture, so drier soils result in more accurate measurements (Desilets et al., 2010; Bogena et al., 2013). In addition, the size of the CRNS detector determines the count rate~~ (~~, i.e., a larger detector volume improves the count statistics and thus reduces the uncertainty of the soil moisture product~~).~~ (Weimar et al., 2020; Schrön et al., 2021b). Different neutron detectors with different sizes and efficiencies are used in this study, so it is important to consider the CRNS-specific uncertainty (e.g., when using the data for validations). Due to the non-linearity of the neutron-soil moisture relationship, the propagated uncertainty $\pm\sigma_\theta$ is highly asymmetric~~.~~ (Iwema et al., 2021). For simplicity, it can be estimated by a symmetrical approximation approach suggested by Jakobi et al. (2020~~).~~):

$$\pm\sigma_\theta = \theta(N) - \theta(N \mp \sigma_N)$$

$$\sigma_\theta \approx \sigma_N \frac{p_2\, N_{\max}}{(N - p_3\, N_{\max})^4} \sqrt{(N - p_3\, N_{\max})^4 + 8\,\sigma_N^2 (N - p_3\, N_{\max})^2 + 15\,\sigma_N^4} \tag{9}$$

where the count rate N follows from the Desilets equation, $\sigma_N = C\sqrt{N_{\mathrm{raw}}}$ is its Gaussian uncertainty, and $p_2 = 0.0752$, $p_3 = 0.346$. We provide both the symmetric and asymmetric uncertainty of the CRNS based soil moisture products in order to facilitate applications where only one of the two options can be used. It is important to note that these stochastic uncertainty estimates do not account for other (systematic) uncertainties, e.g., due to unconsidered biomass effects (Avery et al., 2016), N_0 calibration errors, and unconsidered variations in incoming neutron flux (Baroni et al., 2018), atmospheric pressure (Gugerli et al., 2019), and air humidity~~, etc~~ (Iwema et al., 2021), etc.. Please note that additional uncertainties may have occurred when filling gaps in the air pressure and humidity data with ERA5 data.

Formatiert: Englisch (Vereinigtes Königreich)

3.5 CRNS footprint radius and penetration depth

The footprint radius (i.e., R_{86}) was obtained as the 86% cumulative contribution quantile of the weighting functions from Schrön et al. (2017). For this, we integrated the weights up to 600 m distance considering the influences of soil moisture (as the sum of the CRNS soil moisture, lattice water, and organic carbon), air humidity and pressure. Subsequently, we obtained the average penetration depth (i.e., D_{86}) following Schrön et al. (2017), additionally considering the influence of soil bulk density.

Formatiert: Tiefgestellt

Formatiert: Tiefgestellt

3.6 Normalized quantiles of soil moisture

As suggested by Cooper et al. (2021), we use normalized quantiles to better indicate extreme soil moisture situations. First, the soil moisture values are normalized relative to the minimal and maximal observed soil moisture of the considered time series, i.e., the soil moisture values (θ) are scaled between 0 and 1 (p):

$$p = (\theta - \theta_{min})\,\theta_{max}/\theta_{min}$$

~~$p = (\theta - \theta_{min})/(\theta_{max} - \theta_{min})$~~

(10)

where θ_{min} is the minimum observed soil moisture and θ_{max} is the maximum observed soil moisture. Subsequently, p is used to obtain the quantile represented by each soil moisture value:

~~$Q = \theta_{sort}(p * n)$~~

$$Q = \theta_{sort}(p \cdot n) \qquad (11)$$

where θ_{sort} are the soil moisture values sorted in increasing order and n is the total number of soil moisture observations. From Q the median of all soil moisture values (θ_{med}) is subtracted and the variance is scaled by dividing by the standard deviation (θ_{std}) to obtain the normalized quantiles of soil moisture (Q_{norm}):

~~$Q_{norm} = (Q - \theta_{med})/\theta_{std}$~~

$$Q_{norm} = (Q - \theta_{med})/\theta_{std} \qquad (12)$$

Formatiert: Englisch (Vereinigtes Königreich)

Each Q_{norm} is then plotted against an observed value of the CRNS estimated soil moisture.

3.7 Implementation of the data processing

The raw neutron counts and meteorological data were converted into a uniform data structure (Figure A5b) and stored in a database within the decentralized data infrastructure TEODOOR (TEreno Online Data repOsitORry, Kunkel et al., 2013). The data pre-processing, corrections, calibration and uncertainty estimation were implemented in the programming language Python. These scripts were applied to the raw data stored in the database using ~~NodeRed~~Node-RED, a graphical tool for deploying workflows.~~ NodeRed~~ (Node-RED, 2021). Node-RED offers the possibility to connect different data flows in a simple way, using so-called nodes. Each node has a defined and unique task. When data is transmitted to a node, the node can process these data and then transmit it to the next node. In this way, different corrections or other implementations in the data post-processing can be added or removed individually. As an interface for accessing the data in the TERENO database, the SensorObservationService (SOS) of Open Geospatial Consortium was used. Here, the data is processed by a separate proxy that forwards the requests to a virtual Python environment. In the last step, the processed data was written back directly to the database via email or SOS.

The raw data as well as the processed data are accessible via the TERENO Data Discovery Portal (DDP) at http://www.tereno.net. The data portal enables the query, visualization and access to data and metadata of the stations presented in this paper. Additionally, detailed information on each CRNS station is provided in the metadata (Figure A5a) and can be retrieved from the data portal.

4 Results and Discussion

Formatiert: Schriftfarbe: Automatisch

4.1 Spatiotemporal occurrence of drought events in Europe

The provision of a continental-scale data set on soil moisture dynamics opens up numerous possibilities for analysis, especially with respect to large-scale climatic and hydrological applications. In the following, we present first analyses on the spatiotemporal occurrence of drought events in Europe based on the processed time series of CRNS soil moisture.

Figure 3 visualizes the results of the CRNS soil moisture processing for the COSMOS Europe sites. The CRNS soil moisture (left subplot) show strong temporal variations as well as large differences between the COSMOS-Europe sites. Due to these strong variations in CRNS soil moisture, similarities in the absolute values are difficult to discern, e.g., the impact of large-scale drought events on CRNS soil moisture. Therefore, following the approach of Cooper et al. (2021), Fig. 3 also presents the normalized quantiles of CRNS soil moisture (right subplot) to better indicate extreme soil moisture situations, i.e. to better

Formatiert: Schriftfarbe: Automatisch

distinguish between "normal low" soil moisture and "extremely low" soil moisture. In this way, the widespread impacts on the recent drought events of 2018, 2019 and 2020 on CRNS soil moisture in Europe become more apparent. The 2018 drought, in particular, is clearly visible with pronounced negative values in the normalized soil moisture quantiles across all latitudes, indicating that the whole of Europe was affected by the drought.

In the following, we explore if CRNS soil moisture information can be a valuable basis for more accurate assessment of the uniqueness and potential impacts of drought events at regional to continental scales. In Fig. 4 the monthly mean CRNS soil moisture of all COSMOS-Europe sites since 2011 are presented, along with the spatial mean and STD (upper subplot).

Formatiert: Schriftfarbe: Automatisch

Despite the different time series lengths, the seasonal variations in soil moisture can be clearly seen. We selected three drought events to examine differences in soil moisture between sites, with all data for the period of record presented as normalized quantiles of soil moisture for each site (Fig. 4, lower subplot). It is evident that sites even within the same climate zone with broadly similar weather patterns can have very different ranges and extremes of soil moisture.

This finding confirms results by Cooper et al. (2021) for the United Kingdom, who in particular suggested heterogeneity of soil properties as an explanation for the variabilities, and results of Dong and Ochsner (2018) who found that soil moisture at the regional scale is more controlled by soil texture than precipitation. However, when comparing the three events, it becomes evident that 2018 had more locations with pronounced extremes and that these occurred predominantly in the climate zone Cfb, while 2018 was not notably different from other drought years in the monthly soil moisture averages shown in Fig. 4 (upper subplot). This demonstrates again the advantage of normalized soil moisture quantiles for a more in-depth analysis of extreme events.

Finally, we investigated whether the CRNS data allow us to draw conclusions about longer-term trends in soil moisture in Europe. For this, we contrasted monthly mean soil moisture from 2014 - 2017 with monthly mean soil moisture from 2018 to 2021 in Fig. 5, using the 26 sites fully covering this period. From Fig. 5, it is evident that as of 2018, soil moisture was lower not only in the summer months, but throughout the year. Although the considered soil moisture data covers only 7 years, it can be considered as an indicator of the magnitude and direction of the trend in soil water supply that Europe can expect as climate change progresses.

4.2 How representative and accessible is the soil moisture data?

The representativeness of the individual stations for the depicted land use type and geographical location is relevant, especially with regard to the validation of large-scale model applications of remote sensing products, which usually show coarser spatial resolutions and correspondingly "averaged" representation of site properties (e.g., Colliander et al., 2017; Montzka et al., 2020). In a few cases, the COSMOS-Europe sites represent larger site heterogeneity. This is reflected in particular in the resulting larger variability of soil moisture in the in-situ calibration data measured for the individual sites (see Fig. A4). An example is the CRNS station at the Fürstensee site in Germany~~.~~ (Rasche et al. 2021). The footprint represented by the CRNS measurement at this site includes a sand lens in the center of the footprint, which is surrounded by peat soils. The resulting heterogeneity, particularly of soil properties such as bulk density, soil organic matter content, and lattice water, challenges the harmonized data processing applied for COSMOS-Europe and leads to greater uncertainty in the derived soil moisture product, which are not easy to quantify.

While aspects such as soil heterogeneities or varying land use can be of great importance for local or CRNS-methodological questions, this is rather an obstacle for large-scale questions. Especially with regard to the future development of the European network of CRNS stations, attention should be paid to the selection of sites that guarantee a high representativeness and homogeneity. With respect to the use of COSMOS-Europe data to derive conclusions about continental-scale trends in soil moisture, it is decisive that the network ensures the most representative coverage of key environmental and geographic gradients throughout Europe (e.g., altitude, climate, landforms, geology). This is currently the case only to a limited extent (see also Fig. 1). The clear majority of stations is concentrated in Central Europe, while Scandinavia, Eastern Europe or the

Mediterranean region in particular are covered by only very few stations. This limits the interpretability of the data, especially with regard to comparisons between different climate zones.

Another important question in this context is whether observations at a limited number of points can provide regional improvements in the prediction of hydrologic states and fluxes. For example, Baatz et al. (2017) assimilated measured soil moisture data from a CRNS network into the area-differentiated land surface model CLM 4.5~~ model~~ (Oleson et al., 2013) and showed that updating states and hydraulic parameters leads to better regional hydrologic predictions. This indicates that the COSMOS-Europe data could be beneficial for model applications at the continental scale despite the limited coverage in some areas of Europe, i.e. even though the measurements are not area-wide such as remote sensing data.

Furthermore, at present only a low number of CRNS stations are automatically transferring neutron count data to the TERENO database that hosts the COSMOS-Europe data. However, a near real-time availability of the data would be necessary in particular for the use of the data for the improvement of flood models, e.g., in context of the European Flood Awareness System (EFAS, Smith et al., 2016). Efforts should be made in the future to equip more stations with automatic data transfer capabilities to enable rapid transfer of neutron counts to the TERENO database. Here, the implemented automated routines for data pre-processing, correction and neutron counts to soil moisture allow for immediate provision of COSMOS-Europe data products.

Finally, we would like to point out that there are still alternative data products to some of the CRNS stations used here, which were processed using less comprehensive methods. Although our processing methods closely follow the commonly used method presented by Zreda et al. (2012), there are some important differences as we make use of the latest CRNS research findings from the last 10 years. For example, the US COSMOS database (http://cosmos.hwr.arizona.edu/) does not contain corrections for air humidity, which were suggested by Rosolem et al. (2013) and Köhli et al (2021). Another main difference of our processing scheme is the weighting of the in-situ calibration data according to neutron transport theory (Schrön et al. 2017). We therefore expect soil moisture deviations that can be substantial depending on the date of previous processing schemes.

5 Conclusions and outlook

Formatiert: Schriftfarbe: Automatisch

In this data paper, we present soil moisture data from 65 CRNS stations that are distributed across Europe and cover all major land use types and climate zones. The raw neutron count data from the CRNS stations were processed using state-of-the-art methods in a harmonized way including correction of the raw neutron counts, conversion into soil moisture based on available in-situ information. In addition, information on the data uncertainty is added to the dataset, information that is particularly useful for remote sensing and modelling applications. It should be noted that the sites have individual heterogeneous conditions, which cannot always be adequately reflected by a standard processing scheme. In addition, the data processing used in this work represents the state of the art, but this may change as a result of future research. We therefore provide raw data and will update the published dataset with an incremental version number if new processing procedures become accepted in the future.

We show that the COSMOS-Europe dataset enables a good representation of the magnitude and distribution of drought events. However, so far, only the central part of Europe is particularly well covered by COSMOS-Europe, while there are still large gaps in the peripheral areas of Europe. The density of COSMOS stations in Europe is still not sufficient to completely represent soil moisture patterns across all parts of the continent. Thus, future efforts should invest in higher observational coverage. One emphasis in the further development of COSMOS-Europe must be to convince countries to put CRNS stations into operation that do not yet operate CRNS stations or hardly any. In addition, efforts should be made in the future to equip more stations with automatic data transfer capabilities to enable near real-time accessibility of soil moisture information, e.g., to support flood forecasting. The data presented here can be used for a manifold of hydrological applications, such as drought assessment, flood risk assessment, and snow water estimation.

Similar to COSMOS-Europe, several other large-scale COSMOS networks already exist in the USA, Australia, and India. The obvious next step is to build on the methods developed in this study to create a global network of continental COSMOS networks, similar to the FLUXNET initiative for eddy covariance measurements of land-atmosphere exchange fluxes ~~(https://fluxnet.org/).~~ (FLUXNET, 2021) or the International Soil Moisture Network (ISMN) that provides in situ soil moisture data from 2842 stations worldwide (Dorigo et al., 2021). Initial networking efforts in this direction have already been undertaken.

6 Data access and availability

Formatiert: Schriftfarbe: Automatisch

The dataset, entitled “Dataset of COSMOS-Europe: A European network of Cosmic-Ray Neutron Soil Moisture Sensors”, is stored in a common data format and shared via Forschungszentrum Jülich (https://teodoor.icg.kfa-juelich.de/ibg3butt/ibg.butt.download?FileIdentifier=8e5db846-96d7-491f-9d6c-dbf61423342d, last access: 24 September 2021): https://doi.org/10.34731/x9s3-kr48 (Bogena and Ney, 2021).

Potential users can also access the data of the individual CRNS stations in a dedicated section for COSMOS-Europe in the TERENO data portal TEODOOR at https://ddp.tereno.net/ddp/dispatch?searchparams=keywords-Cosmic%20Ray. Here, both metadata information about the stations (e.g., site owner) as well as the raw data and the processed data products can be accessed. Please note that downloads will only be made possible via a token and are provided with a disclaimer with the terms of use.

Formatiert: Schriftfarbe: Automatisch

Formatiert: Schriftfarbe: Automatisch

7 Acknowledgements

Formatiert: Schriftfarbe: Automatisch

We thank TERENO (Terrestrial Environmental Observatories), funded by the Helmholtz-Gemeinschaft for the financing and maintenance of CRNS stations and the NMDB database funded by EU-FP7 for providing incoming neutron data. We acknowledge support by the Deutsche Forschungsgemeinschaft (DFG, German Research Foundation), project 357874777 of the research unit FOR 2694 Cosmic Sense and by the German Federal Ministry of Education and Research (BMBF), BioökonomieREVIER, Digitales Geosystem-Rheinisches Revier (DG-RR).

We thank Peter Strauss and Gerhab Rab from the Institute for Land and Water Management Research, Federal Agency for Water Management Austria, Petzenkirchen, Austria. We thank Trenton Franz from School of Natural Resources, University of Nebraska-Lincoln, Lincoln, NE, United States. We also thank Carmen Zengerle, Mandy Kasner, ~~and~~ Felix Pohl, and Solveig Landmark, UFZ Leipzig, for supporting field calibration, lab analysis, and data processing. We furthermore thank Daniel Dolfus, Marius Schmidt, Ansgar Weuthen and Bernd Schilling, Forschungszentrum Jülich, Germany.

COSMOS-UK has been supported financially by the UK’s Natural Environment Research Council (grant no. NE/R016429/1). The COSMOS-UK project team is thanked for making its data available to COSMOS-Europe. Dr. Luca Stevanato is thanked for the technical details about the Finapp sensor.

The stations at Cunnersdorf, Lindenberg, and Harzgerode have been supported by Falk Böttcher and Frank Beyrich, German Weather Service (DWD). The Zerbst site has been supported by Getec Green Energy GmbH. The Olocau experimental watershed is partially supported by the Spanish Ministry of Science and Innovation through the research project TETISCHANGE (ref. RTI2018-093717-B-I00). Calderona experimental site is partially supported by the Spanish Ministry of Science and Innovation through the research projects CEHYRFO-MED (CGL2017-86839-C3-2-R) and SILVADAPT.NET (RED2018-102719-T), and the LIFE project RESILIENT FORESTS (LIFE17 CCA/ES/000063). University of Bristol’s Sheepdrove sites have been supported by the UK’s Natural Environment Research Council through a number of projects (grants NE/M003086/1, NE/ R004897/1, and NE/T005645/1) and by the International Atomic Energy Agency of the United

Formatiert: Englisch (Vereinigte Staaten)

Formatiert: Englisch (Vereinigte Staaten)

Formatiert: Englisch (Vereinigte Staaten)

Formatiert: Englisch (Vereinigte Staaten)

Nations (project CRP D12014). CESBIO's sites have been supported by the CNES TOSCA programme. The ERA5-Land data are provided by ECMWF (Muñoz Sabater, 2021).

Formatiert: Schriftart: +Überschriften (Times New Roman)

References

Formatiert: Schriftfarbe: Automatisch

~~Miller, B. B. and Carter, C.: The test article, J. Sci. Res., 12, 135–147, doi:10.1234/56789, 2015.~~

~~Smith, A. A., Carter, C., and Miller, B. B.: More test articles, J. Adv. Res., 35, 13–28, doi:10.2345/67890, 2014.~~

Andreasen, M., Jensen, K. H., Desilets, D., Franz, T., Zreda, M., Bogena, H., and Looms, M.C.: Status and perspectives of the cosmic-ray neutron method for soil moisture estimation and other environmental science applications. Vadose Zone J., 16(8), doi:10.2136/vzj2017.04.0086, 2017a.

Andreasen, M., Jensen, K. H., Desilets, D., Zreda, M., Bogena, H., and Looms, M.C.: Cosmic-ray neutron transport at a forest field site: the sensitivity to various environmental conditions with focus on biomass and canopy interception. Hydrol. Earth Syst. Sci., 21, 1875–1894, doi:10.5194/hess-21-1875-201, 2017b.

Andreasen, M., ~~Looms, M.C., and Jensen, K.H.: Cosmic-ray neutron intensity and soil moisture estimates in the period 2013–2019 at three field sites located in the western part of Denmark. PANGAEA, doi:10.1594/PANGAEA.909271, 2019.~~

~~Andreasen, M.,~~ Jensen, K.H., Bogena, H., Desilets, D., Zreda, M., and Looms, M.C.: Cosmic ray neutron soil moisture estimation using physically based site-specific conversion functions. Water Resources Research, 56, e2019WR026588, doi:10.1029/2019WR026588, 2020.

Andreasen, M., Looms, M.C., and Jensen, K.H.: Cosmic-ray neutron intensity and soil moisture estimates in the period 2013–2019 at three field sites located in the western part of Denmark. PANGAEA, doi:10.1594/PANGAEA.909271, 2019.

Baatz, R., Bogena, H. R., Hendricks Franssen, H.-J., Huisman, J. A., Montzka, C., and Vereecken, H.: An empirical vegetation correction for soil moisture content quantification using cosmic ray probes. Water Resour. Res., 51, 2030–2046, doi:10.1002/2014WR016443, 2015.

Baatz, R., Bogena, H.R., Hendricks Franssen, H.J., Huisman, J.A., Qu, W., Montzka, C., and Vereecken, H.: Calibration of a catchment scale cosmic-ray probe network: A comparison of three parameterization methods. J. Hydrol., 516, 231-244, doi:10.1016/j.jhydrol.2014.02.026, 2014.

Baroni, G., Scheiffele, L. M., Schrön, M., Ingwersen, J. and Oswald, S.E.: Uncertainty, sensitivity and improvements in soil moisture estimation with cosmic-ray neutron sensing. J. Hydrol., 564, 873–887, doi:10.1016/j.jhydrol.2018.07.053, 2018.

Beck, H.E., Zimmermann, N.E., McVicar, T.R., Vergopolan, N., Berg, A. and Wood E.F.: Present and future Köppen-Geiger climate classification maps at 1-km resolution. Sci. Data., 5, 180214, doi:10.1038/sdata.2018.214, 2018.

Berthelin, R., Rinderer, M., Andreo, B., Baker, A., Kilian, D., Leonhardt, G., Lotz, A., Lichtenwoehrer, K., Mudarra, M., Y. Padilla, I., Pantoja Agreda, F., Rosolem, R., Vale, A., and Hartmann, A.: A soil moisture monitoring network to characterize karstic recharge and evapotranspiration at five representative sites across the globe. Geoscientific Instrumentation, Methods and Data Systems, 9(1), 11–23, doi:10.5194/gi-9-11-2020, 2020.

Blöschl, G., Blaschke, A. P., Broer, M., Bucher, C., Carr, G., Chen, X., Eder, A., Exner-Kittridge, M., Farnleitner, A., Flores-Orozco, A., Haas, P., Hogan, P., Kazemi Amiri, A., Oismüller, M., Parajka, J., Silasari, R., Stadler, P., Strauss, P., Vreugdenhil, M., Wagner, W., and Zessner, M.: The Hydrological Open Air Laboratory (HOAL) in Petzenkirchen: a hypothesis-driven observatory, Hydrol. Earth Syst. Sci., 20, 227–255, doi:10.5194/hess-20-227-2016, 2016.

Bogena, H., and Ney, P.: Dataset of "COSMOS-Europe: A European network of Cosmic-Ray Neutron Soil Moisture Sensors", ~~orschungszentrum~~Forschungszentrum Jülich, https://doi.org/10.34731/x9s3-kr48, 2021.

~~Bogena, H.R., Huisman, J. A., Baatz, R., Hendricks Franssen, H.-J., and Vereecken, H.: Accuracy of the cosmic-ray soil water content probe in humid forest ecosystems: The worst case scenario. Water Resour. Res., 49, 1–14, doi:10.1002/wrcr.20463, 2013.~~

~~Bogena, H.R., Montzka, C., Huisman, J.A., Graf, A., Schmidt, M., Stockinger, M., et al.: The Rur Hydrological Observatory: A multiscale multi-compartment research platform for the advancement of hydrological science. Vadose Zone J., 17, 180055, doi:10.2136/vzj2018.03.0055, 2018.~~

Bogena, H.R., Herrmann, F., Jakobi, J., Brogi, C., Ilias, A., Huisman, J.A., Panagopoulos, A., and Pisinaras, V.: Monitoring of Snowpack Dynamics With Cosmic-Ray Neutron Probes: A Comparison of Four Conversion Methods. Front. Water, 2:19, doi:10.3389/frwa.2020.00019, 2020.

Bogena, H.R., Huisman, J. A., Baatz, R., Hendricks Franssen, H.-J., and Vereecken, H.: Accuracy of the cosmic-ray soil water content probe in humid forest ecosystems: The worst case scenario. Water Resour. Res., 49, 1–14, doi:10.1002/wrcr.20463, 2013.

Bogena, H.R., Huisman, J.A., Güntner, A., Hübner, C., Kusche, J., Jonard, F., Vey, S., and Vereecken, H.: Emerging methods for noninvasive sensing of soil moisture dynamics from field to catchment scale: A review. Wiley Interdisciplinary Reviews: Water 2(6), 635-647, doi:10.1002/wat2.1097, 2015.

Bogena, H.R., Montzka, C., Huisman, J.A., Graf, A., Schmidt, M., Stockinger, M., et al.: The Rur Hydrological Observatory: A multiscale multi-compartment research platform for the advancement of hydrological science. Vadose Zone J., 17, 180055, doi:10.2136/vzj2018.03.0055, 2018.

Colliander, A., Jackson, T. J., Bindlish, R., Chan, S., Das, N., Kim, S. B., et al.: Validation of SMAP surface soil moisture products with core validation sites. Remote Sensing of Environment, 191, 215-231, 2017.

Cooper, H. M., Bennett, E., Blake, J., Blyth, E., Boorman, D., Cooper, E., et al.: COSMOS-UK: national soil moisture and hydrometeorology data for environmental science research. Earth System Science Data, 13(4), 1737-1757, 2021.

Desilets, D., and Zreda, M.: Spatial and temporal distribution of secondary cosmic-ray nucleon intensities and applications to in situ cosmogenic dating. Earth and Planetary Science Letters, 206(1-2), 21-42, 2003.

Desilets, D., Zreda, M., and Ferré, T.P.A.: Nature´s neutron probe: Land surface hydrology at an elusive scale with cosmic rays. Water Resour. Res., 46, W11505, doi:10.1029/2009WR008726, 2010.

Dimitrova-Petrova, K., Geris, J., Wilkinson, M.E., Lilly, A., and Soulsby, C.: Using isotopes to understand the evolution of water ages in disturbed mixed land-use catchments. Hydrol. Proc., 34(4), 972-990, doi:10.1002/hyp.13627, 2020b.

Dimitrova-Petrova, K., Geris, J., Wilkinson, M.E., Rosolem, R., Verrot, L., Lilly, A., and Soulsby, C.: Opportunities and challenges in using catchment-scale storage estimates from cosmic ray neutron sensors for rainfall-runoff modelling. J. Hydrol., 586, 124878, 2020a.

Dimitrova-Petrova, K., ~~Geris, J., Wilkinson, M.E., Lilly, A., and Soulsby, C.: Using isotopes to understand the evolution of water ages in disturbed mixed land-use catchments. Hydrol. Proc., 34(4), 972-990, doi:10.1002/hyp.13627, 2020b.~~

~~Dimitrova-Petrova, K.,~~ Rosolem, R., Soulsby, C., Wilkinson, M.E., Lilly, A., and Geris J.: Combining static and portable Cosmic Ray Neutron Sensor data to assess catchment scale heterogeneity in soil water storage and their integrated role in catchment runoff response. J. Hydrol., 126659, doi:10.1016/j.jhydrol.2021.126659, 2021.

Dong, J., and Ochsner, T. E.: Soil texture often exerts a stronger influence than precipitation on mesoscale soil moisture patterns. Water Resour. Res., 54, 2199–2211, doi:10.1002/2017WR021692, 2018.

Dorigo, W., Himmelbauer, I., Aberer, D., Schremmer, L., Petrakovic, I., Zappa, L., ... and Sabia, R.: The International Soil Moisture Network: serving Earth system science for over a decade. Hydrol. Earth Syst. Sci., 25, 5749-5804, doi: 10.5194/hess-25-5749-2021, 2021.

DWD: Lindenberg Meteorological Observatory – Richard Assmann Observatory. https://www.dwd.de/SharedDocs/broschueren/EN/press/mo_lindenberg_en.pdf?__blob=publicationFile&v=3 (last viewed 10 September 2021), 2021.

Formatiert: Englisch (Vereinigtes Königreich)

Formatiert: Englisch (Vereinigtes Königreich)

Evans, J. G., Ward, H. C., Blake, J. R., Hewitt, E. J. Morrison, R., Fry, M., et al.: Soil water content in southern England derived from a cosmic ray soil moisture observing system: COSMOS-UK. Hydrol. Process., 30, 4987–4999, doi:10.1002/hyp.10929, 2016.

Fersch, B., Francke, T., Heistermann, M., Schrön, M., Döpper, V., Jakobi, J. et al.: A dense network of cosmic-ray neutron sensors for soil moisture observation in a highly instrumented pre-Alpine headwater catchment in Germany. Earth System Science Data, 12(3), 2289-2309, 2020.

Fink, A. H., Brücher, T., Krüger, A., Leckebusch, G. C., Pinto, J. G., and Ulbrich, U.: The 2003 European summer heatwaves and drought-synoptic diagnosis and impacts. Weather, 59(8), 209–216, 2004.

Fischer, C., Tischer, J., Roscher, C. et al.: Plant species diversity affects infiltration capacity in an experimental grassland through changes in soil properties. Plant Soil, 397, 1~~–~~-16,~~-~~ doi:10.1007/s11104-014-2373-5, 2015.

FLUXNET: The data portal serving the FLUXNET community. https://fluxnet.org/ (last viewed 10 December 2021) 2021.

Franz, T. E., Wahbi, A., Vreugdenhil, M., Weltin, G., Heng, L., Oismueller, M., Strauss, P., Dercon, G. and Desilets, D.: Using cosmic-ray neutron probes to monitor landscape scale soil water content in mixed land use agricultural systems. Applied and Environmental Soil Science, 2016, doi:10.1155/2016/4323742, 2016.

Franz, T. E., Wahbi, A., Zhang, J., Vreugdenhil, M., Heng, L., Dercon, G., and Wagner, W.: Practical data products from cosmic-ray neutron sensing for hydrological applications. Frontiers in Water, 2(9), doi:10.3389/frwa.2020.00009, 2020.

Franz, T. E., Zreda, M., Rosolem, R., and Ferre, T.P.A.: Field validation of a cosmic-ray neutron sensor using a distributed sensor network. Vadose Zone J. 11(4), doi:10.2136/vzj2012.0046, 2012.

~~Franz, T. E., Wahbi, A., Vreugdenhil, M., Weltin, G., Heng, L., Oismueller, M., Strauss, P., Dercon, G. and Desilets, D.: Using cosmic-ray neutron probes to monitor landscape scale soil water content in mixed land use agricultural systems. Applied and Environmental Soil Science, 2016, doi:10.1155/2016/4323742, 2016.~~

Franz, T.E., Wahbi, A., Zhang, J., Vreugdenhil, M., Heng, L., Dercon, G., Strauss, P., Brocca, L. and Wagner, W.: Practical Data Products From Cosmic-Ray Neutron Sensing for Hydrological Applications. Front. Water, 2~~:~~, 9 doi:10.3389/frwa.2020.00009, 2020.

Gardner, W., and Kirkham, D.: Determination of soil moisture by neutron scattering. Soil Science, 73(5), 391-402, 1952.

González-Sanchis, M., García-Soro, J. M., Molina, A. J., Lidón, A. L., Bautista, I., Rouzic, E., et al.: Comparison of soil water estimates from cosmic-ray neutron and capacity sensors in a semi-arid pine forest: Which is able to better assess the role of environmental conditions and thinning?. Front. Water, 2, 39, 2020.

Graf, A., Klosterhalfen, A., Arriga, N., Bernhofer, C., Bogena, H., Bornet, F. et al.: Altered energy partitioning across terrestrial ecosystems in the European drought year 2018. Philosophical Transactions of the Royal Society B, 375(1810), 20190524, 2020.

Grumm, R.H.: The central European and Russian heat event of July-August 2010. BAMS, 1285–1296, doi:10.1175/2011BAMS3174.1., 2011.

Hanel, M., Rakovec, O., Markonis, Y., Máca, P., Samaniego, L., Kyselý, J., and Kumar, R.: Revisiting the recent European droughts from a long-term perspective. Scientific Reports, 8(1), 9499, 2018.

Hawdon, A., McJannet, D., and Wallace, J. Calibration and correction procedures for cosmic-ray neutron soil moisture probes located across Australia. Water Resour. Res., 50, 5029–5043, doi:10.1002/2013WR015138, 2014.

Heidbüchel, I., Güntner, A., and Blume, T.: Use of cosmic-ray neutron sensors for soil moisture monitoring in forests. Hydrology and Earth System Sciences 20(3), 1269-1288, 2016.

Heinrich, I., Balanzategui, D., Bens, O., Blasch, G., Blume, T., Böttcher, F., et al.: Interdisciplinary geo-ecological research across time scales in the Northeast German Lowland Observatory (TERENO-NE). Vadose Zone J., 17(1), 2018.

Hengl, T., Mendes de Jesus, J., Heuvelink, G. B., Ruiperez Gonzalez, M., Kilibarda, M., Blagotić, A., et al.: SoilGrids250m: Global gridded soil information based on machine learning. PLoS one, 12(2), e0169748, 2017

Humphrey, V., Berg, A., Ciais, P. et al.: Soil moisture–atmosphere feedback dominates land carbon uptake variability. Nature 592, 65–69, doi:10.1038/s41586-021-03325-5, 2021.

Ionita, M., Tallaksen, L., Kingston, D., Stagge, J., Laaha, G., Van Lanen, H., et al.: The European 2015 drought from a climatological perspective. Hydrology and Earth System Sciences, 21, 1397–1419, 2017.

Iwema, J.: Opportunities and Limitations of the Cosmic-Ray Neutron Soil Moisture Sensor under Humid Conditions. PhD-thesis, University of Bristol, UK, 2017.

Iwema, J., Schrön, M., Koltermann Da Silva, J., Schweiser De Paiva Lopes, R., and Rosolem, R.: Accuracy and precision of the cosmic-ray neutron sensor for soil moisture estimation at humid environments. Hydrological Processes, 35(11), e14419. https://doi.org/10.1002/hyp.14419, 2021.

Jakobi, J., Huisman, J.A., Schrön, M., Fiedler, J., Brogi, C., and Bogena, H.: Error estimation~~ with~~ for soil moisture measurements from with cosmic-ray neutron sensing and with implications for rover surveys. Front. Water, 2:10, doi:10.3389/frwa.2020.00010, 2020~~, 2020~~.

Jakobi, J., Huisman, J.A., Vereecken, H., Diekkrüger, B., and Bogena H.R.: Cosmic-ray neutron sensing for simultaneous soil water content and biomass quantification in drought conditions. Water Resour. Res., 54(10), 7383-7402, doi: 10.1029/2018WR022692, 2018.

Kelley, C.P., Mohtadi, S., Cane, M. A., Seager, R., and Kushnir, Y.: Climate change in the Fertile Crescent and implications of the recent Syrian drought. Proceedings of the National Academy of Sciences, 3241–3246, 2015.

Kiese, R., Fersch, B., Baessler, C., Brosy, C., Butterbach-Bahl, K., Chwala, C., et al.: The TERENO Pre-Alpine Observatory: Integrating meteorological, hydrological and biogeochemical measurements and modeling. Vadose Zone J., 17:180060, doi:10.2136/vzj2018.03.0060, 2018.

Köhli, M., Schrön, M., Zreda, M., Schmidt, U., Dietrich, P., and Zacharias, S.: Footprint characteristics revised for field-scale soil moisture monitoring with cosmic-ray neutrons. Water Resour. Res., 51(7), 5772-5790, doi:10.1002/2015WR017169, 2015.

Köhli, M., Weimar, J., Schrön, M., and Schmidt, U.: ~~Moisture~~Soil moisture and air humidity dependence of the above-ground cosmic-ray neutron intensity. Front. Water, 2, 544847, doi:10.3389/frwa.2020.544847, 2020.

Kunkel, R., Sorg, J., Eckardt, R., Kolditz, O., Rink, K., Vereecken, H.: TEODOOR: a distributed geodata infrastructure for terrestrial observation data. Environmental Earth Sciences, 2, 507-521, doi:10.1007/s1266501323707, 2013.

Laaha, G., Gauster, T., Tallaksen, L.M., Vidal, J.-P., Stahl, K., Prudhomme, C., et al.: The European 2015 drought from a hydrological perspective. Hydrology and Earth System Sciences, 21, 3001–3024, 2017.

Li, D., Schrön, M., Köhli, M., Bogena, H., Weimar, J., Bello, M.A.J., Han, X., Gimeno, M.A.M., Zacharias, S., Vereecken, H., and Hendricks Franssen, H.-J.: Can drip irrigation be scheduled with a cosmic-ray neutron sensor? Vadose Zone J., 18(1), 190053. doi:10.2136/vzj2019.05.0053, 2019.

Miller, B. B. and Carter, C.: The test article, J. Sci. Res., 12, 135–147, doi:10.1234/56789, 2015.

~~Montzka, C., Bogena, H.R., Zreda, M., Monerris, A., Morrison, R., Muddu, S., and Vereecken, H.: Validation of spaceborne and modelled surface soil moisture products with cosmic-ray neutron probes. Remote Sensing, 9(2), 103, 2017.~~

Montzka, C., Bogena, H.R., Herbst, M., Cosh, M. H., Jagdhuber, T., and Vereecken, H.: Estimating the number of reference sites necessary for the validation of global soil moisture products. IEEE Geoscience and Remote Sensing Letters, 18(9), 1530-1534, doi:10.1109/LGRS.2020.3005730, 2020.

Montzka, C., Bogena, H.R., Zreda, M., Monerris, A., Morrison, R., Muddu, S., and Vereecken, H.: Validation of spaceborne and modelled surface soil moisture products with cosmic-ray neutron probes. Remote Sensing, 9(2), 103, 2017.

Muñoz Sabater, J.: ERA5-Land hourly data from 1950 to 1980, Copernicus Climate Change Service (C3S) Climate Data Store (CDS) [data set], https://doi.org/10.24381/cds.e2161bac, 2021.

Formatiert: Englisch (Vereinigte Staaten)

Formatiert: Englisch (Vereinigte Staaten)

Nasta, P., Bogena, H. R., Sica, B., Weuthen, A., Vereecken, H., and Romano, N.: Integrating Invasive and Non-invasive Monitoring Sensors to Detect Field-Scale Soil Hydrological Behavior. Front. Water, 2, 26, doi:10.3389/frwa.2020.00026, 2020.

Ney, P., Köhli, M., Bogena, H., and Goergen, K.: CRNS-based monitoring technologies for a weather and climate-resilient agriculture: realization by the ADAPTER project. 2021 IEEE International Workshop on Metrology for Agriculture and Forestry (MetroAgriFor), 203-208, doi: 10.1109/MetroAgriFor52389.2021.9628766, 2021.

Node-RED. Node-RED documentation, https://nodered.org/docs/user-guide/. (2021, December)

Oleson, K., Lawrence, D.M., Bonan, G.B., Drewniak, B., Huang, M., Koven, C.D. et al.: Technical description of version 4.5 of the Community Land Model (CLM). Tech. Note NCAR/TN-503+STR. Natl. Ctr. Atmos. Res., Boulder, CO, 2013.

Otkin, J.A., Anderson, M. C., Hain, C., Svoboda, M., Johnson, D., Mueller, R., et al.: Assessing the evolution of soil moisture and vegetation conditions during the 2012 United States flash drought. Agricultural and Forest Meteorology, 218, 230–242, 2016.

Patil, A., Fersch, B., Hendricks Franssen, H.J., and Kunstmann, H.: Assimilation of Cosmogenic Neutron Counts for Improved Soil Moisture Prediction in a Distributed Land Surface Model. Front. Water, 3, 115, doi: 10.3389/frwa.2021.729592, 2021.

Pisinaras, V., Panagopoulos, A., Herrmann, F., Bogena, H.R., Doulgeris, C., Ilias, A., Tziritis, E., and Wendland, F.: Hydrologic and geochemical research at Pinios Hydrologic Observatory - Initial results. Vadose Zone J., 17(1), doi: 10.2136/vzj2018.05.0102, 2018.

Power, D., Rico-Ramirez, M. A., Desilets, S., Desilets, D., and Rosolem, R.: Cosmic-Ray neutron Sensor PYthon tool (crspy): Cosmic-Ray neutron Sensor PYthon tool (crspy 1.2.1): an open-source tool for the processing of cosmic-ray neutron and soil moisture data. Geoscientific Model Development, 14(12), 7287-7307, 2021.

Rasche, D., Köhli, M., Schrön, M., Blume, T., and Güntner, A.: Towards disentangling heterogeneous soil moisture patterns in cosmic-ray neutron sensor footprints, Hydrol. Earth Syst. Sci., 25, 6547–6566, https://doi.org/10.5194/hess-25-6547-2021, 2021.

Rivera Villarreyes, C.A., Baroni, G., and Oswald, S.E.: Integral quantification of seasonal soil moisture changes in farmland by cosmic-ray neutrons. Hydrol. Earth Syst. Sci., 15(12), 3843-3859, 2011.

Romano, N., Nasta, P., Bogena, H., De Vita, P., Stellato, L., and Vereecken, H.: Monitoring hydrological processes for land and water resources management in a Mediterranean ecosystem: The Alento River Catchment Observatory. Vadose Zone J., 17(1), 1-12, 2018.

~~Power, D., Rico-Ramirez, M. A., Desilets, S., Desilets, D., and Rosolem, R.: Cosmic-Ray neutron Sensor PYthon tool (crspy): An open-source tool for the processing of cosmic-ray neutron and soil moisture data. Geoscientific Model Development Discussions, 1-34, 2021.~~

Schattan, P., Baroni, G., Oswald, S. E., Schöber, J., Fey, C., Kormann, C., Huttenlau, M., and Achleitner, S.: Continuous monitoring of snowpack dynamics in alpine terrain by aboveground neutron sensing. Water Resour. Res., 53(5), 3615–3634, doi:10.1002/2016WR020234, 2017.

Schattan, P., Köhli, M., Schrön, M., Baroni, G., and Oswald, S. E~~. (2019a).~~.: Sensing Area-Average Snow Water Equivalent with Cosmic-Ray Neutrons: The Influence of Fractional Snow Cover. Water Resour. Res., 5~~–~~(12), 10796-10812, doi:10.1029/2019WR025647, 2019a.

Schattan, P., Baroni, G., and Oswald, S.E.: Cosmic-Ray Neutron Data at the Weisssee Snow Research Site. PANGAEA, doi:10.1594/PANGAEA.900959, 2019b.

Schattan, P., Schwaizer, G., Schöber, J., and Achleitner, S.: The complementary value of cosmic-ray neutron sensing and snow covered area products for snow hydrological modelling. Remote Sensing of Environment, 239, 111603, 2020.

Schrön, M., Köhli, M., Scheiffele, L., Iwema, J., Bogena, H.R., Lv, L., Martini, E., Baroni, G., Rosolem, R., Weimar, J., Mai, J., Cuntz, M., Rebmann, C., Oswald, S. E., Dietrich, P., Schmidt, U., and Zacharias, S.: Spatial sensitivity of cosmic-ray

Formatiert: Englisch (Vereinigte Staaten)

neutron sensors applied to improve calibration and validation. Hydrol. Earth Syst. Sci., 21, 5009–5030, doi:10.5194/hess-21-5009-2017, 2017.

Schrön, M., Oswald, S. E., Zacharias, S., Kasner, M., Dietrich, P., and Attinger, S.: Neutrons on Rails–trans-regional monitoring of soil moisture and snow water equivalent. Geophysical Research Letters, e2021GL093924, doi:10.1029/2021gl093924, 2021b.

Schrön, M., Zacharias, S., Köhli, M., Weimar, J. and Dietrich, P.: Monitoring environmental water with ground albedo neutrons and correction for incoming cosmic rays with neutron monitor data. In: The 34th International Cosmic Ray Conference, 30 July- 6 August, 2015. The Hague, The Netherlands (ICRC2015) vol. 236 231 (Proceedings of Science, 2016), doi:10.22323/1.236.0231, 2015.

Schrön, M., Zacharias, S., Womack, G., Köhli, M., Desilets, D., Oswald, S. E., Bumberger, J, Mollenhauer H., Kögler, S., Remmler, P., Kasner, M., Denk, A. and Dietrich, P.: Intercomparison of cosmic-ray neutron sensors and water balance monitoring in an urban environment. Geoscientific Instrumentation, Methods and Data Systems, 7(1), 83-99, 2018.

Schrön, M.: CORNish PASDy -- COsmic-Ray Neutron flavored PASDy PASDy -- Processing and Analysis of Sensor Data in pYthon. https://git.ufz.de/CRNS/cornish_pasdy (2021a, December 16)

Schuldt, B., Buras, A., Arend, M., Vitasse, Y., Beierkuhnlein, C., Damm, A., et al.: A first assessment of the impact of the extreme 2018 summer drought on Central European forests. Basic and Applied Ecology, 45, 86-103, 2020.

Seneviratne, S.I., Lehner, I., Gurtz, J., Teuling, A.J., Lang, H., Moser, U., Grebner, D., Menzel, L., Schroff, K., Vitvar, T., and Zappa, M.: Swiss prealpine Rietholzbach research catchment and lysimeter: 32 year time series and 2003 drought event. Water Resour. Res., 48, W06526, doi:10.1029/2011WR011749, 2012.

Smith, A. A., Carter, C., and Miller, B. B.: More test articles, J. Adv. Res., 35, 13–28, doi:10.2345/67890, 2014.

Smith, P. J., Pappenberger, F., Wetterhall, F., Del Pozo, J. T., Krzeminski, B., Salamon, P., et al.: On the operational implementation of the European Flood Awareness System (EFAS). In: Flood forecasting, 313-348, Academic Press, 2016.

Stott, P.A., Stone, D.A., and Allen, M.R.: Human contribution to the European heatwave of 2003. Nature, 432, 610–614, doi:10.1038/nature03130, 2004.

Sutanto, S.J., Vitolo, C., Di Napoli, C., D'Andrea, M., and Van Lanen, H.A.: Heatwaves, droughts, and fires: exploring compound and cascading dry hazards at the pan-European scale. Environment International, 134, 105276, 2020.

Topp, G.C., Davis, J.L., and Annan, A.P. Electromagnetic determination of soil water content: Measurements in coaxial transmission lines. Water Resour. Res., 16, 574–582, 1980.

Turco, M., von Hardenberg, J., AghaKouchak, A., Carmen Llasat, M., Provenzale, A., and Trigo, R.M.: On the key role of droughts in the dynamics of summer fires in mediterranean Europe. Scient. Rep., 7, 81, doi:10.1038/s41598-017-00116-9, 2017.

van Dijk, A.I.J.M., Beck, H.E., Crosbie, R.S., de Jeu, R.A.M., Liu, Y.Y., Podger, G.M., et al.: The millennium drought in southeast Australia (2001-2009): Natural and human causes and implications for water resources, ecosystems, economy, and society. Water Resources Research, 49, 1040–1057, doi:10.1002/wrcr.20123, 2013.

Vather, T., Everson, C.S., and Franz, T.E.: The Applicability of the Cosmic Ray Neutron Sensor to Simultaneously Monitor Soil Water Content and Biomass in an Acacia mearnsii Forest. Hydrology, 7(3), 48, 2020.

Weimar, J., Köhli, M., Budach, C. and Schmidt, U.: Large-Scale Boron-Lined Neutron Detection Systems as a 3He Alternative for Cosmic Ray Neutron Sensing. Frontiers Water, 2, 16, 2020.

Wollschläger, U., Attinger, S., Borchardt, D., Brauns, M., Cuntz, M., Dietrich, P., ... ~~&~~and Zacharias, S. (2017). The Bode hydrological observatory: a platform for integrated, interdisciplinary hydro-ecological research within the TERENO Harz/Central German Lowland Observatory. Environmental Earth Sciences, 76(1), 1-25.

Yiou, P., Cattiaux, J., Faranda, D., Kadygrov, N., Jézéquel, A., Naveau, P., et al.: Analyses of the Northern European summer heatwave of 2018. Bulletin of the American Meteorological Society, 101(1), S35-S40, 2020.

Formatiert: Englisch (Vereinigtes Königreich)

Formatiert: Englisch (Vereinigte Staaten)

Formatiert: Deutsch (Deutschland)

Zreda, M., Desilets, D., Ferre, T.P.A., and Scott, R.L.: Measuring soil moisture content non-invasively at intermediate spatial scale using cosmic-ray neutrons. Geophys. Res. Lett., 35, L21402, doi:10.1029/2008GL035655, 2008.

Zreda, M., W. J. Shuttleworth, X. Zeng, C. Zweck, D. Desilets, T. Franz, and R. Rosolem: COSMOS: The COsmic-ray Soil Moisture Observing System. Hydrol. Earth Syst. Sci., 16, 4079–4099, doi:10.5194/hess-16-4079-2012, 2012.

Zreda, M., Nitychoruk, J., Chodyka, M., Świerczewska-Pietras, K., and Zbucki, Ł.: New method for measuring soil moisture using cosmogenic neutrons. Prz. Geol., 63/4: 239–246, 2015.

Tables

Table 1: General information of the COSMOS-Europe sites (ordered based on latitude)

Station	Country	Affiliation	Detector	Geographic coordinates		Alt.	Main land use	Mean air temp.	Mean annual precip.	Climate class.	Time period	
				lat	lon	(m)		(°C)	(mm)		start	end
Aas[1]	Norway, NO	NVE		59.664	10.762	72	Grassland	6.2*	1240*	Dfb	09.2016	07.2021
Saerheim[1]	Norway, NO	NVE		58.761	5.651	91	Grassland	7.7*	2500*	Cfb	09.2017	07.2021
Elsick[8]	Scotland,GB	Uni Aberdeen	CRS1000/B	57.039	-2.186	95	Cropland	12.0	800	Cfb	11.2015	12.2020
Glensaugh[6]	Scotland, GB	COSMOS-UK	CRS2000/B	56.914	-2.562	399	Moorland	7.0	1109	Cfb	05.2014	06.2021
Gludsted[2]	Denmark, DK	HOBE	CRS1000/B	56.071	9.334	86	Plantation	8.2	1050	Dfb	02.2013	06.2021
Voulund[2]	Denmark,DK	HOBE	CRS1000/B	56.036	9.156	67	Cropland	8.2	1050	Dfb	02.2013	06.2021
Harrild[2]	Denmark, DK	HOBE	CRS1000/B	56.022	9.155	66	Heathland	8.2	1050	Dfb	03.2014	06.2021
Serrahn[7]	Germany, DE	TERENO/GFZ	CRS1000	53.339	13.174	96	Forest	9.7*	580	Dfb	08.2016	12.2020
Wildacker[7]	Germany, DE	TERENO/GFZ	CRS1000	53.330	13.199	96	Forest	9.7*	580	Dfb	07.2013	12.2020
Fuerstensee[7]	Germany, DE	TERENO/GFZ	CRS1000	53.319	13.122	66	Grassland	9.7*	580	Dfb	01.2014	01.2021
Fincham[6]	England, GB	COSMOS-UK	CRS2000/B	52.618	0.511	15	Cropland	10.5*	613	Cfb	06.2017	06.2021
Euston[6]	England, GB	COSMOS-UK	CRS2000/B	52.383	0.785	18	Grassland	10.0	600	Cfb	03.2016	06.2021
Derlo	Poland, PL	Uni Warsaw	CRS1000	52.170	23.369	129	Grassland	7.5	550	Dfb	04.2013	06.2021
Lindenberg	Germany, DE	UFZ	CRS2000	52.165	14.121	72	Grassland	9.2	576	Dfb	06.2020	today
Hohes Holz[7]	Germany, DE	TERENO/UFZ	CRS2000/B	52.090	11.226	217	Forest	10.0*	820*	Dfb	08.2014	today
Grosses Bruch[7]	Germany, DE	TERENO/UFZ	CRS1000	52.030	11.105	80	Cropland	9.9*	845*	Dfb	07.2014	today
Hordorf[7]	Germany, DE	TERENO/UFZ	CRS1000	51.997	11.179	82	Cropland	10.0*	818*	Dfb	06.2020	today
Zerbst	Germany, DE	UFZ	2x CRS1000	51.993	12.126	74	Grassland	10.4*	847*	Dfb	06.2020	today
Schaefertal1	Germany, DE	Uni Potsdam	CRS1000	51.657	11.043	425	Cropland	9.9*	951*	Dfb	10.2010	09.2019
~~Schaefertal3~~	~~Germany, DE~~	~~Uni Potsdam~~	~~CRS1000~~	~~51.655~~	~~11.052~~	~~394~~	~~Cropland~~	~~9.9*~~	~~951*~~	~~Dfb~~	~~10.2011~~	~~05.2019~~
Schaefertal4	Germany, DE	Uni Potsdam	CRS1000	51.655	11.049	399	Cropland	9.9*	951*	Dfb	09.2010	06.2020
Harzgerode[7]	Germany, DE	TERENO/UFZ	CRS2000	51.652	11.137	405	Grassland	7.6	582	Dfb	11.2019	05.2021
Sheepdrove2[5]	England, GB	Uni Bristol	CRS 2000/B	51.528	-1.468	204	Cropland	9.5	815	Cfb	06.2015	12.2019

Formatiert ...
Formatierte Tabelle ...
Formatiert ...
Formatiert ...
Formatiert ...
Formatiert ...
Formatiert ...
Formatiert ...
Formatiert ...
Formatiert ...
Formatiert ...
Formatiert ...
Formatiert ...
Formatiert ...
Formatiert ...
Formatiert ...
Formatiert ...
Formatiert ...
Formatiert ...
Formatiert ...
Formatiert ...
Formatiert ...
Formatiert ...
Formatiert ...
Formatiert ...
Formatiert ...
Formatiert ...
Formatiert ...
Formatiert ...
Formatiert ...
Formatiert ...
Formatiert ...
Formatiert ...
Formatiert ...
Formatiert ...
Formatiert ...
Formatiert ...
Formatiert ...
Formatiert ...
Formatiert ...
Formatiert ...
Formatiert ...
Formatiert ...
Formatiert ...

Station	Country	Affiliation	Detector	Geographic coordinates		Alt.	Main land use	Mean air temp.	Mean annual precip.	Climate class.	Time period	
				lat	lon	(m)		(°C)	(mm)		start	end
Sheepdrove3[5]	England, GB	Uni Bristol	CRS 2000/B	51.523	-1.486	182	Cropland	9.5	815	Cfb	07.2015	07.2019
Sheepdrove1[5]	England, GB	Uni Bristol	CRS 2000/B	51.515	-1.458	197	Cropland	9.5	815	Cfb	07.2015	12.2019
Cunnersdorf	Germany, DE	UFZ	CRS1000	51.370	12.557	140	Cropland	10.5*	868*	Dfb	06.2016	today
Wildenrath[7]	Germany, DE	TERENO/FZJ	CRS1000	51.133	6.169	72	Forest	10.3	722	Cfb	04.2012	today
Heinsberg[7]	Germany, DE	TERENO/FZJ	CRS1000	51.041	6.104	58	Cropland	10.3	722	Cfb	09.2011	today
Gevenich[7]	Germany, DE	TERENO/FZJ	CRS1000	50.989	6.324	107	Cropland	10.3	718	Cfb	07.2011	today
Jena	Germany, DE	Uni Potsdam	CRS2000/B	50.951	11.625	140	Grassland	9.9	612	Dfb	03.2015	11.2017
Merzenhausen[7]	Germany, DE	TERENO/FZJ	CRS1000	50.930	6.297	91	Cropland	10.3	718	Cfb	02.2011	today
Selhausen[7]	Germany, DE	TERENO/FZJ	CRS2000/B	50.866	6.447	101	Cropland	10.3	718	Cfb	03.2015	today
Ruraue[7]	Germany, DE	TERENO/FZJ	CRS1000	50.862	6.427	100	Grassland	10.3	718	Cfb	11.2011	today
Boernchen	Germany, DE	GFZ	CRS2000/B	50.819	13.800	571	Cropland	8.9*	986*	Dfb	06.2019	06.2021
Aachen[7]	Germany, DE	TERENO/FZJ	CRS1000	50.799	6.025	232	Cropland	10.3	865	Cfb	01.2012	today
Lullington[6]	England, GB	COSMOS-UK	CRS2000/B	50.794	0.189	199	Heath	10.0	825	Cfb	12.2014	06.2021
Bornheim[9]	Germany, DE	ADAPTER/FZJ	Styx V1	50.785	6.956	67	Cropland	10.8*	1071*	Cfb	10.2020	today
Noervenich[9]	Germany, DE	ADAPTER/FZJ	Styx V1	50.781	6.537	140	Cropland	10.5*	1030*	Cfb	11.2020	today
~~Kleinhau[7]~~Kleinhau1[7]	Germany, DE	TERENO/FZJ	CRS2000B	50.722	6.372	374	Grassland	9.0	614	Cfb	08.2015	today
Kleinhau2[15]	Germany, DE	MOSES/FZJ	CRS2000B	50.718	6.399	394	Reforestation	9.0	614	Cfb	06.2020	today
Zuelpich[9]	Germany, DE	ADAPTER/FZJ	Styx V1	50.692	6.717	158	Cropland	10.4*	1009*	Cfb	09.2020	today
Rollesbroich2[7]	Germany, DE	TERENO/FZJ	CRS1000	50.624	6.305	506	Grassland	7.0	1018	Dfb	07.2012	today
Rollesbroich1[7]	Germany, DE	TERENO/FZJ	CRS1000	50.622	6.304	515	Grassland	7.0	1018	Dfb	05.2011	today
Schoeneseiffen[7]	Germany, DE	TERENO/FZJ	CRS2000B	50.515	6.376	611	Grassland	7.0	870	Dfb	08.2015	today
Wuestebach2[7]	Germany, DE	TERENO/FZJ	CRS2000B	50.505	6.331	607	Forest	7.0	1180	Dfb	06.2014	today
Wuestebach1[7]	Germany, DE	TERENO/FZJ	CRS1000	50.503	6.333	605	Forest	7.0	1180	Dfb	02.2011	today
Wuestebach3[7]	Germany, DE	TERENO/FZJ	CRS2000B	50.503	6.336	605	Reforestation	7.0	1180	Dfb	03.2020	today

Formatiert
Formatierte Tabelle
Formatiert
Formatiert
Formatiert
Formatiert
Formatiert
Formatiert
Formatiert
Formatiert
Formatiert
Formatiert
Formatiert
Formatiert
Formatiert
Formatiert
Formatiert
Formatiert
Formatiert
Formatiert
Formatiert
Formatiert
Formatiert
Formatiert
Formatiert
Formatiert
Formatiert
Formatiert
Formatiert
Formatiert
Formatiert
Formatiert
Formatiert
Formatiert
Formatiert
Formatiert
Formatiert
Formatiert
Formatiert
Formatiert
Formatiert
Formatiert
Formatiert
Formatiert

Kall[7]	Germany, DE	TERENO/FZJ	CRS1000	50.501	6.526	505	Grassland	8.0	857	Dfb	09.2011	today

Station	Country	Affiliation	Detector	Geographic coordinates		Alt.	Main land use	Mean air temp.	Mean annual precip.	Climate class.	Time period	
				lat	lon	(m)		(°C)	(mm)		start	end
Petzenkirchen[4]	Austria, AT	IAEA	CRS1000/B	48.155	15.148	278	Cropland	10.0*	1065*	Dfb	12.2013	today
Fendt[7]	Germany, DE	TERENO/KIT	CRS2000/B	47.832	11.060	595	Gassland	8.4*	1630*	Dfb	06.2015	03.2021
Acheleschwaig[7]	Germany, DE	TERENO/KIT	CRS2000/B	47.666	10.994	867	Grassland	7.0*	1805*	Dfb	06.2017	03.2021
Graswang[7]	Germany, DE	TERENO/KIT	CRS2000/B	47.571	11.033	863	Grassland	5.4*	1948*	Dfb	06.2017	03.2021
Esterberg[7]	Germany, DE	TERENO/KIT	CRS2000/B	47.516	11.158	1267	Grassland	4.3*	2062*	Dfc	06.2017	03.2021
Zugspitze[12]	Germany, DE	UFZ	CRS1000	47.416	10.979	2900	Bare rock/Glacier	-4.3	2085	ET	10.2015	today
Rietholzbach	Switzerland, CH	ETH Zürich	CRS1000	47.381	8.993	755	Grassland	7.1	1460	Dfb	12.2010	02.2020
Leutasch[3]	Austria, AT	Uni Innsbruck	CRS2000/B	47.376	11.162	1111	Grassland	4.0*	2155*	Dfc	12.2018	today
Weisssee[3]	Austria, AT	Uni Innsbruck	CRS1000, CRS2000/B	46.873	10.714	2464	Sparse Vegetation	-2.7*	1547*	ET	02.2014	today
Crolles	France, FR	CESBIO	CRS1000	45.281	5.901	230	Grassland	7.5	900	Cfb	07.2016	06.2018
Toulouse	France, FR	CESBIO	CRS1000	43.385	1.292	188	Grassland	13.6	1028*	Cfa	02.2011	08.2018
Bussoleno	Italy, IT	Uni Polit Turin	FINAPP	45.118	7.162	625	Forest	12.6	792	Cfb	11.2020	today
Alento2[10]	Italy, IT	Uni Napoli	CRS2000/B	40.365	15.184	453	Orchard	15.4	1215	Csa	02.2016	08.2021
Alento1[10]	Italy, IT	Uni Napoli	CRS2000/B	40.311	15.229	671	Forest	13.6	1255	Csa	02.2016	08.2021
Agia[14]	Greece, GR	PHO	CRS2000/B	39.755	22.717	1032	Shrubland	12.5	1003	Csb	03.2017	today
Olocau	Spain, ES	UFZ	CRS1000	39.707	-0.517	415	Shrubland	16.2*	544*	BSk	01.2017	09.2020
Calderona1	Spain, ES	Uni Valencia	CRS2000/B	39.708	-0.457	785	Shrubland	16.6*	525*	BSk	10.2016	06.2021
Calderona2	Spain, ES	Uni Valencia	CRS2000/B	39.708	-0.457	789	Shrubland	16.6*	525*	BSk	07.2019	06.2021
Cakit Basin[13]	Turkey, TR	METU	CRS2000/B	37.515	34.498	1459	Shrubland	9.8	338	BSk	11.2016	07.2019

*derived from ERA5 data

[1] part of the groundwater and soil moisture monitoring network of the Norwegian water resources and energy directorate operated since 1998 and 1999, respectively.

[2] part of The Danish Hydrological Observatory, HOBE (www.hobe.dk). Data is partly published by Andreasen et al. (2019; 2020) with more information on the field sites.

[3] part of the Moosbeere network operated by the University of Innsbruck. The Weisssee station is located on rocky terrain and not suited for soil moisture analysis.

[4] part of the Hydrological Open-Air Laboratory HOAL (https://hoal.hydrology.at/the-hoal), which is a cooperation project between the Federal Agency for Water Management (BAW Petzenkirchen) and the Technical University Vienna. More information about the site can be found in Blöschl et al. (2016)

[5] located at the Sheepdrove Organic Farm in the UK. More information about the site can be found in Iwema ~~(2017; Chapter 5~~et al. (2021), Schrön et al. (2017) and Berthelin et al. (2020)

[6] part of the COSMOS-UK network operated by the UK Centre for Ecology & Hydrology. Further information about the sites and COSMOS-UK is presented in Cooper et al. (2021)

Formatiert ...
Formatiert ...
Formatiert ...
Formatiert ...
Formatiert ...
Formatiert ...
Formatiert ...
Formatiert ...
Formatiert ...
Formatiert ...
Formatiert ...
Formatiert ...
Formatiert ...
Formatiert ...
Formatiert ...
Formatiert ...
Formatiert ...
Formatiert ...
Formatiert ...
Formatiert ...
Formatiert ...
Formatiert ...
Formatiert ...
Formatiert ...
Formatiert ...
Formatiert ...
Formatierte Tabelle ...
Formatiert ...
Formatiert ...
Formatiert ...
Formatiert ...
Formatiert ...
Formatiert ...
Formatiert ...
Formatiert ...
Formatiert ...
Formatiert ...
Formatiert ...
Formatiert ...
Formatiert ...
Formatiert ...
Formatiert ...
Formatiert ...
Formatiert

[7] part of the German Terrestrial Environmental Observatories (TERENO) network (www.tereno.net).

[8] the CRNS is placed at the corner of three adjacent agricultural fields.Further information about the site can be found Dimitrova-Petrova et al. (2020a; 2020b; 2021)

[9] part of the ADAPTER (ADAPT TERrestrial systems) project (www.adapter-projekt.de), Ney et al. (2021)

[10] part of Alento Hydrological Observatory (AHO) in southern Italy established in 2016 by the University of Naples in cooperation with Forschungszentrum Jülich GmbH (Romano et al., 2018; Nasta et al., 2020).

[11] due to a malfunction, the detector had to be replaced. To ensure a consistent time series, the neutron counts 1 year before and after the replacement were compared and the time series after the replacement were adjusted accordingly.

[12] The Zugspitze sensor is located in the Schneefernerhaus (UFS) observatory and surrounded by rocky mountain terrain and not suited for soil moisture analysis.

[13] operated by the Water Resources Lab. of Middle East Technical University

[14] part of Pinios Hydrologic Observatory (PHO) in central Greece established in 2017 by the Soil & Water Resources Institute, Hellenic Agricultural Organization "DEMETER" in cooperation with Forschungszentrum Jülich GmbH (Pisinaras et al., 2018; Bogena et al., 2020).

[15] part of the MOSES (Modular Observation Solutions for Earth Systems) project (https://www.ufz.de/moses/)

Formatiert: Schriftfarbe: Automatisch

Formatiert: Schriftfarbe: Automatisch

Formatiert: Schriftfarbe: Automatisch

Formatiert: Schriftfarbe: Automatisch

Formatiert: Schriftfarbe: Automatisch

Formatiert: Schriftfarbe: Automatisch

Formatiert: Schriftfarbe: Automatisch

Formatiert: Schriftfarbe: Automatisch

Formatiert: Schriftfarbe: Automatisch

Formatiert: Schriftfarbe: Automatisch

Formatiert: Schriftfarbe: Automatisch

Formatiert: Schriftfarbe: Automatisch

Formatiert: Schriftfarbe: Automatisch

Table 2: Physical quantities of the COSMOS-Europe sites

Station	Porosity	Bulk density* (g/cm³)	Soil organic carbon* (g/g)	Lattice water* (g/g)	Cutoff rigidity (GV)	N0 (cts/h)	Mean raw epithermal neutrons (cts/h)	Mean corrected epithermal neutrons (cts/h)	Mean soil moisture (m³/m³)	Soil moisture range (m³/m³)	Mean Footprint depth (m)	Mean Footprint radius (m)	References
Aas, NO	0.~~589~~579	1.~~088~~029	-0.082[1]	-0.034[1]	1.21	~~2448~~2788	1744	~~1483~~1484	0.~~218~~227	0.~~111~~058 - 0.~~345~~463	0.256	155.6	-
Saerheim, NO	0.~~559~~496	1.~~169~~146	-0.150[1]	-0.016[1]	1.31	~~2552~~2861	1863	1552	0.~~261~~218	0.~~104~~00 - 0.~~394~~455	0.229	146.8	-
Elsick, GB	0.587	0.997	0.094	0.032	1.61	3071	1828	1537	0.392	0.124 - 0.587	0.187	118.7	Dimitrova-Petrova et al. (2020a)
Glensaugh, GB	0.838	0.356	0.182	0.012	1.59	2807	1834	1185	0.469	0.200 - 0.837	0.464	121.6	Cooper et al. (2021)
Gludsted, DK	0.637	0.814	0.163	0.002	1.87	1560	849	778	0.297	0.059 - 0.634	0.243	120.5	Andreasen et al. (2019, 2020)
Voulund, DK	0.453	1.388	0.045	0.004	1.87	1677	1135	1078	0.187	0.000 - 0.361	0.208	155.3	Andreasen et al. (2019, 2020)
Harrild, DK	0.642	0.873	0.086	0.001	1.87	1423	792	715	0.383	0.028 - 0.642	0.228	121.1	Andreasen et al. (2019, 2020)
Serrahn, DE	0592	1.014	0.064	0.002	2.50	769	551	491	0.124	0.013 - 0.285	0.326	168.8	Heinrich et al. (2018)
Wildacker, DE	0.577	1.095	0.025	0.003	2.50	799	613	563	0.115	0.009 - 0.245	0.368	183.4	Heidbüchel et al. (2016)
Fuerstensee, DE	0.559	1.135	0.031	0.002	2.51	1085	794	740	0.134	0.011 - 0.323	0.326	174.5	Heinrich et al. (2018)
Fincham, GB	0.507	1.283	0.019	0.007	2.65	2655	1785	1656	0.236	0.091 - 0.346	0.213	147.7	Cooper et al. (2021)
Euston, GB	0.529	1.214	0.029	0.003	2.69	2667	1951	1833	0.145	0.003 - 0.280	0.301	174.0	Cooper et al. (2021)
Derlo, PL	0.~~458~~453	1.~~436~~430	-0.015[1]	0.043	2.79	~~1108~~1128	846	756	0.~~143~~136	0.~~009~~000 - 0.~~346~~352	0.232	168.1	Zreda et al. (2015)
Lindenberg, DE	0.~~393~~442	1.~~600~~454	0.~~005~~019[1]	0.~~020~~012[1]	2.80	~~2585~~1999	~~1640~~1643	~~1448~~1461	0.~~226~~136	0.~~094~~000 - 0.~~393~~298	0.~~128~~263	~~128.5~~173.1	~~DWD (2021)~~-
Hohes Holz, DE	0.~~908~~905	0.~~244~~243	-0.031[1]	0.005	2.81	~~938~~946	561	~~458~~459	0.~~145~~143	0.~~052~~046 - 0.~~272~~283	~~1.556~~0.326	~~184~~168.8	Wollschläger et al. (2017)
Grosses Bruch, DE	0.~~651~~560	~~0.925~~1.126	-0.037[1]	0.~~038~~048	2.85	~~796~~903	568	516	0.~~129~~233	0.~~054 – 0209~~086 – 0.410	0.~~381~~215	~~178~~134.2	Wollschläger et al. (2017)
Hordorf, DE	0.~~473~~506	1.~~397~~278	-0.025[1]	0.~~041~~043[1]	2.87	~~1018~~1067	~~699~~700	~~623~~625	0.~~252~~249	0.~~087~~074 - 0.~~447~~475	0.~~181~~190	~~139.8~~135.2	-
Zerbst, DE	0.~~430~~438	1.~~427~~408	0.058	-0.018[1]	2.81	~~1109~~1141	865	755	0.~~127~~130	0.000 - 0.~~224~~231	0.~~224~~211	~~168.3~~162.1	-
Schaefertal1, DE	0.537	1.185	0.037	0.010	2.91	1168	985	675	0.233	0.058 - 0.536	0.216	146.1	Wollschläger et al. (2017)

Formatiert ...
Formatierte Tabelle ...
Formatiert ...
Formatiert ...
Formatiert ...
Formatiert ...
Formatiert ...
Formatiert ...
Formatiert ...
Formatiert ...
Formatiert ...
Formatiert ...
Formatiert ...
Formatiert ...
Formatiert ...
Formatiert ...
Formatiert ...
Formatiert ...
Formatiert ...
Formatiert ...
Formatiert ...
Formatiert ...
Formatiert ...
Formatiert ...
Formatiert ...
Formatiert ...
Formatiert ...
Formatiert ...
Formatiert ...
Formatiert ...
Formatiert ...
Formatiert ...
Formatiert ...
Formatiert ...
Formatiert ...
Formatiert ...
Formatiert ...
Formatiert ...
Formatiert ...
Formatiert ...
Formatiert ...
Formatiert ...
Formatiert ...
Formatiert ...

Schaefertal4, DE	0.607	1.010	0.033	0.010	2.91	968	906	618	0.143	0.000 - 0.606	0.327	174.4	Wollschläger et al. (2017)
Harzgerode, DE	0.~~393~~506	1.~~600~~282	0.~~005~~021^1	0.~~0040~~047^1	2.97	~~1892~~2013	~~1820~~1774	~~1208~~1169	0.~~280~~253	0.~~160~~093 - 0.~~393~~423	0.~~157~~188	~~143.0~~139.2	-
Sheepdrove2, GB	0.566	1.100	0.046	0.031	2.90	2724	1774	1425	0.385	0.197 - 0.566	0.180	119.7	Iwema et al. (~~2017~~2021)
Sheepdrove3, GB	0.586	1.048	0.046	0.031	2.90	2698	1683	1377	0.419	0.213 - 0.~~585~~586	0.182	118.8	Iwema et al. (~~2017~~2021)
Sheepdrove1, GB	0.480	1.335	0.033	0.031	2.90	2636	1818	1471	0.348	0.174 - 0.480	0.158	122.3	Iwema et al. (~~2017~~2021)

Station	Porosity	Bulk density* (g/cm³)	Soil organic carbon* (g/g)	Lattice water* (g/g)	Cutoff rigidity (GV)	N0 (cts/h)	Mean raw epithermal neutrons (cts/h)	Mean corrected epithermal neutrons (cts/h)	Mean soil moisture (m³/m³)	Soil moisture range (m³/m³)	Mean Footprint depth (m)	Mean Footprint radius (m)	References
Cunnersdorf, DE	0.~~393~~428	1.~~600~~491	0.~~005~~018	0.~~0040~~030	2.94	~~1134~~1079	~~810~~808	~~700~~699	0.~~255~~201	0.~~082~~004 - 0.~~393~~424	0.~~156~~198	~~137.6~~151.2	-
Wildenrath, DE	0.565	1.126	0.025	0.002	2.98	964	684	628	0.173	0.039 - 0.375	0.290	166.9	Bogena et al. (2018)
Heinsberg, DE	0.530	1.215	0.026	0.010	3.03	1192	725	713	0.259	0.064 - 0.440	0.211	138.8	Bogena et al. (2018)
Gevenich, DE	0.496	1.318	0.014	0.013	3.04	1158	782	715	0.257	0.056 - 0.496	0.215	127.2	Bogena et al. (2018)
Jena, DE	0.482	1.340	0.025	0.028	3.09	~~2223~~2229	1621	1432	0.~~172~~175	0.~~064~~065 - 0.~~241~~245	0.220	159.6	Fischer et al (2015)
Merzenhausen, DE	0.500	1.310	0.012	0.015	3.09	1143	767	715	0.238	0.063 - 0.440	0.210	147.6	Bogena et al. (2018)
Selhausen, DE	0.514	1.276	0.010	0.023	3.10	997	652	583	0.295	0.081 - 0.514	0.186	132.8	Bogena et al. (2018)
Ruraue, DE	0.575	1.102	0.022	0.020	3.05	1049	665	598	0.286	0.071 - 0.526	0.220	134.5	Bogena et al. (2018)
Boernchen, DE	0.592	1.037	0.042	0.006	3.10	2762	2811	1599	0.222	0.080 - 0.410	0.250	150.6	-
Aachen, DE	0.571	1.112	0.023	0.033	3.15	1134	764	605	0.369	0.147 - 0.570	0.185	122.9	Bogena et al. (2018)
Lullington, GB	0.676	0.821	0.047	0.005	3.03	2524	1515	1329	0.308	0.125 - 0.643	0.280	129.3	Cooper et al. (2021)
Bornheim, DE	0.513	1.276	0.011	0.021	3.07	2343	1503	1350	0.303	0.151 - 0.513	0.181	133.1	-
Noervenich, DE	0.524	1.250	0.010	0.019	3.15	2195	1673	1380	0.213	0.123 - 0.346	0.225	155.9	-
~~Kleinhau~~Kleinhau1, DE	0.599	1.019	0.042	0.030	3.09	905	710	493	0.296	0.078 - 0.478	0.221	131.9	Bogena et al. (2018)
Kleinhau2, DE	0.622	0.897	0.110	0.024	3.09	2576	1965	1286	0.341	0.183 – 0.545	0.215	122.5	
Zuelpich, DE	0.487	1.343	0.012	0.016	3.12	1920	1403	1190	0.247	0.062 - 0.348	0.196	145.7	-
Rollesbroich2, DE	0.623	0.944	0.058	0.027	3.19	1043	855	536	0.347	0.121 - 0.623	0.215	127.2	Bogena et al. (2018)

Formatiert ...
Formatiert ...
Formatiert ...
Formatiert ...
Formatiert ...
Formatiert ...
Formatiert ...
Formatiert ...
Formatiert ...
Formatiert ...
Formatiert ...
Formatiert ...
Formatiert ...
Formatiert ...
Formatiert ...
Formatiert ...
Formatiert ...
Formatiert ...
Formatiert ...
Formatiert ...
Formatiert ...
Formatiert ...
Formatiert ...
Formatiert ...
Formatiert ...
Formatiert ...
Formatiert ...
Formatiert ...
Formatiert ...
Formatiert ...
Formatiert ...
Formatiert ...
Formatiert ...
Formatiert ...
Formatiert ...
Formatiert ...
Formatiert ...
Formatiert ...
Formatiert ...
Formatiert ...
Formatiert ...
Formatiert ...
Formatiert ...
Formatiert ...

Rollesbroich1, DE	0.596	1.032	0.039	0.032	3.10	1146	936	600	0.352	0.094 - 0-595	0.199	126.9	Bogena et al. (2018)
Schoeneseiffen, DE	0.609	1.000	0.038	0.036	3.19	950	897	504	0.305	0.111 - 0.519	0.214	131.8	Bogena et al. (2018)
Wuestebach2, DE	0.832	0.417	0.070	0.024	3.28	2530	1910	1110	0.388	0.209 - 0.831	0.457	124.3	Bogena et al. (2018)
Wuestebach1, DE	0.713	0.697	0.088	0.025	3.28	1289	853	608	0.395	0.204 - 0.688	0.265	123.5	Bogena et al. (2018)
Wuestebach3, DE	0.687	0.770	0.078	0.028	3.28	866	763	415	0.392	0.238 - 0.616	0.242	123.4	Bogena et al. (2018)
Kall, DE	0.625	0.959	0.038	0.037	3.22	1262	984	662	0.319	0.135 - 0.604	0.221	128.3	Bogena et al. 2018
Petzenkirchen, AT	0.501	1.317	0.004	0.039	4.06	1344	986	750	0.352	0.154 - 0.501	0.159	125.2	Franz et al. (2016, 2020)
Fendt, DE	0.719	0.725	0.030	0.011	4.08	2318	1937	1127	0.384	0.242 - 0.535	0.277	124.7	Fersch et al. (2020)

Station	Porosity	Bulk density*	Soil organic carbon*	Lattice water*	Cutoff rigidity	N0	Mean raw epithermal neutrons	Mean corrected epithermal neutrons	Mean soil moisture	Soil moisture range	Mean Footprint depth	Mean Footprint radius	References
		(g/cm³)	(g/g)	(g/g)	(GV)	(cts/h)	(cts/h)	(cts/h)	(m³/m³)	(m³/m³)	(m)	(m)	
Acheleschwaig, DE	0.658	0.853	0.063	0.023	4.15	2333	2557	1163	0.337	0.161 - 0.466	0.233	128.8	-
Graswang, DE	0.728	0.690	0.045	0.037	4.23	2335	2308	1052	0.474	0.303 - 0.613	0.253	125.3	Kiese et al. (2018)
Esterberg, DE	0.757	0.567	0.125	0.094	4.25	2213	2870	933	0.520	0.324 - 0.699	0.272	130.8	-
Zugspitze, DE	-	-	-	-	4.17	-	-	-	-	-	-	-	-
Rietholzbach, CH	0.617	0.964	0.052	0.032	4.22	1150	1101	569	0.397	0.162 - 0.589	0.194	126.2	Seneviratne et al. (2012)
Leutasch, AT	~~-~~0.552	~~-~~1.120[1]	~~-~~0.060[1]	~~-~~0.051[1]	4.28	~~1258~~117	751	~~701~~60	0.~~270~~252	0.~~148 -~~ 0.~~352~~79 - 0.643	0.227	188.6	Schattan et al. (2019a,b)
Weisssee, AT	~~-~~0.562	~~-~~1.110[1]	~~-~~0.047[1]	~~-~~0.031[1]	4.42	~~968~~1103	3971	521	0.~~054~~070	0.~~012~~000 - 0.~~129~~152	0.467	232.4	Schattan et al. (2019a,b)
Crolles, FR	0.368	1.612	0.040	0.039	4.90	928	671	538	0.262	0.035 - 0.368	0.133	127.5	-
Toulouse, FR	0.486	1.354	0.008	0.030	5.51	890	706	623	0.139	0.013 - 0.311	0.27	174.8	-
Bussoleno, IT	0.521	1.230[1]	0.032[1]	0.052[1]	4.72	2158	2524	1302	0.193	0.057 – 0.410	0.218	152.6	-
Alento2, IT	0.560	1.126	0.037	0.055	6.87	2029	1743	1153	0.243	0.070 - 0.475	0.212	135.4	Nasta et al. (2020)
Alento1, IT	0.652	0.858	0.075	0.036	6.87	1814	1739	971	0.243	0.091 - 0.479	0.268	134.2	Nasta et al. (2020)
Agia, GR	0.~~519~~511	1.~~275~~258	~~-~~0.031[1]	0.~~058~~059	7.17	~~1917~~1988	2948	1183	0.210	0.~~070~~052 - 0.~~513~~511	0.216	165.2	Pisinaras et al. (2018)
Olocau, ES	0.453	1.426	0.017	0.005	7.36	777	757	~~559~~558	0.~~143~~144	0.010 - 0.321	0.258	182.6	-
Calderona1, ES	0.542	1.177	0.032	0.006	7.36	1980	2420	1251	0.193	0.112 - 0.400	0.251	166.7	González-Sanchis et al. (2020)

Calderona2, ES	0.~~520~~514	1.~~271~~252	-0.029[1]	-0.042[1]	7.36	~~803~~871	1013	515	0.~~240~~237	0.~~151~~117 - 0.~~437~~507	0.226	161.6	González-Sanchis et al. (2020)
Cakit Basin, TR	0.~~440~~443	1.485	-0.014[1]	-0.054[1]	8.37	~~1634~~1798	3826	1103	0.~~191~~177	0.~~106~~061 - 0.~~338~~391	0.202	185.8	Duygu and Akyürek (2019)

* weighted after Schrön et al., 2017

[1] from SoilGrids

Formatiert: Schriftfarbe: Automatisch

Formatiert: Schriftfarbe: Automatisch

Formatiert: Schriftfarbe: Automatisch

Formatiert: Schriftfarbe: Automatisch

Formatiert: Schriftfarbe: Automatisch

Formatiert: Schriftfarbe: Automatisch

Formatiert: Schriftfarbe: Automatisch

Formatiert: Schriftfarbe: Automatisch

Formatiert: Schriftfarbe: Automatisch

Formatiert: Schriftfarbe: Automatisch

Formatiert: Schriftfarbe: Automatisch

Formatiert: Schriftfarbe: Automatisch

Formatiert: Schriftfarbe: Automatisch

Formatiert: Schriftfarbe: Automatisch

Formatiert: Schriftfarbe: Automatisch

Formatiert: Schriftfarbe: Automatisch

Formatiert: Schriftfarbe: Automatisch

Formatiert: Schriftfarbe: Automatisch

Formatiert: Schriftfarbe: Automatisch

Formatiert: Schriftfarbe: Automatisch

Formatiert: Schriftfarbe: Automatisch

Formatiert: Schriftfarbe: Automatisch

Formatiert: Schriftfarbe: Automatisch

Formatiert: Schriftfarbe: Automatisch

Formatiert: Schriftfarbe: Automatisch

Figures

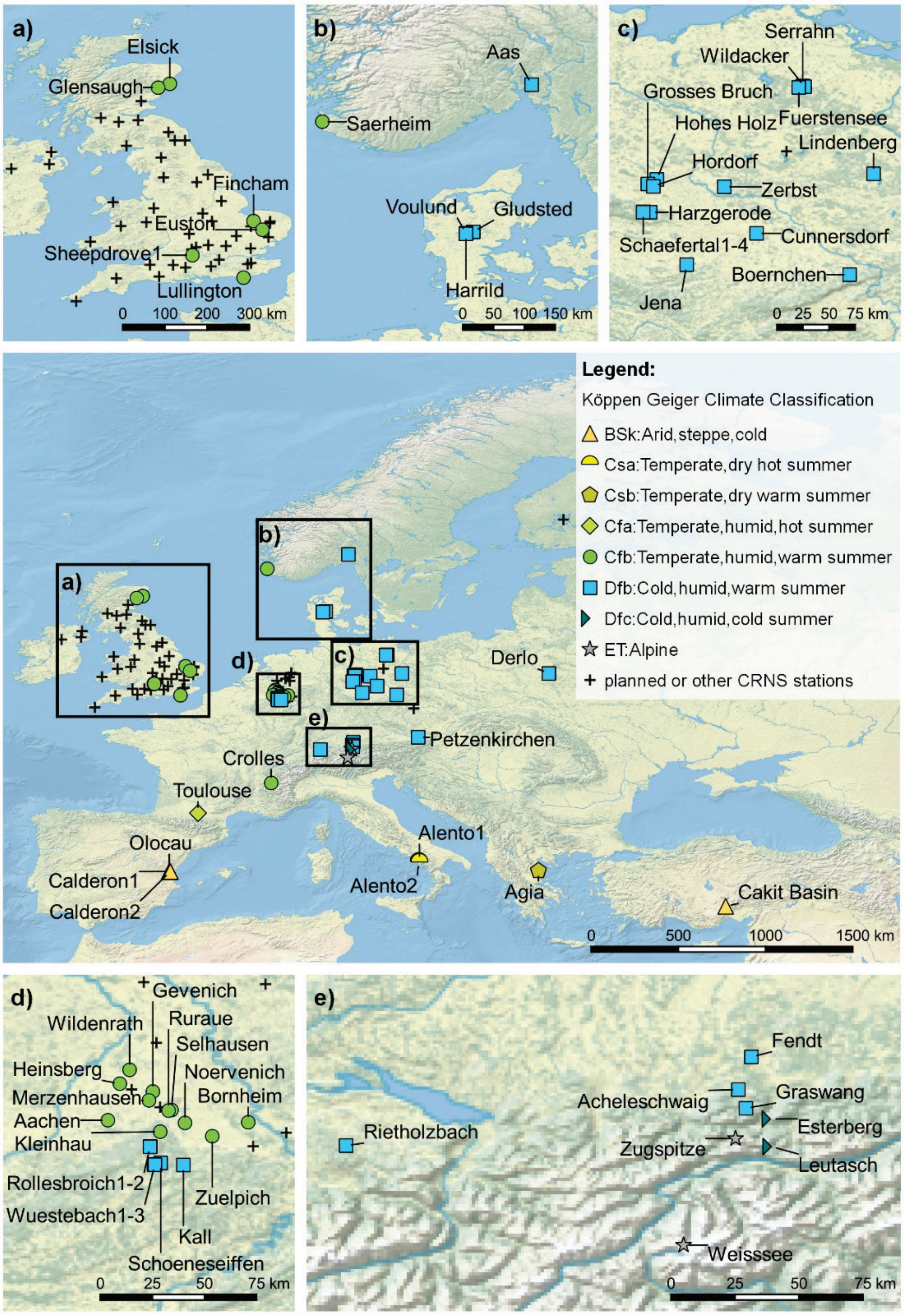
a)
Elsick
Glensaugh
Fincham
Euston
Sheepdrove1
Lullington
0 100 200 300 km
b)
Aas
Saerheim
Voulund
Gludsted
Harrild
0 50 100 150 km
c)
Serrahn
Wildacker
Grosses Bruch
Hohes Holz
Fuerstensee
Lindenberg
Hordorf
Zerbst
Harzgerode
Schaefertal1-4
Cunnersdorf
Boernchen
Jena
0 25 50 75 km
Legend:
Köppen Geiger Climate Classification
BSk:Arid,steppe,cold
Csa:Temperate,dry hot summer
Csb:Temperate,dry warm summer
Cfa:Temperate,humid,hot summer
Cfb:Temperate,humid,warm summer
Dfb:Cold,humid,warm summer
Dfc:Cold,humid,cold summer
ET:Alpine
planned or other CRNS stations
a)
b)
c)
d)
e)
Derlo
Petzenkirchen
Crolles
Toulouse
Olocau
Calderon1
Calderon2
Alento1
Alento2
Agia
Cakit Basin
0 500 1000 1500 km
d)
Gevenich
Wildenrath
Ruraue
Selhausen
Heinsberg
Noervenich
Merzenhausen
Bornheim
Aachen
Kleinhau
Rollesbroich1-2
Wuestebach1-3
Zuelpich
Kall
Schoeneseiffen
0 25 50 75 km
e)
Fendt
Acheleschwaig
Graswang
Esterberg
Rietholzbach
Zugspitze
Leutasch
Weisssee
0 25 50 75 km

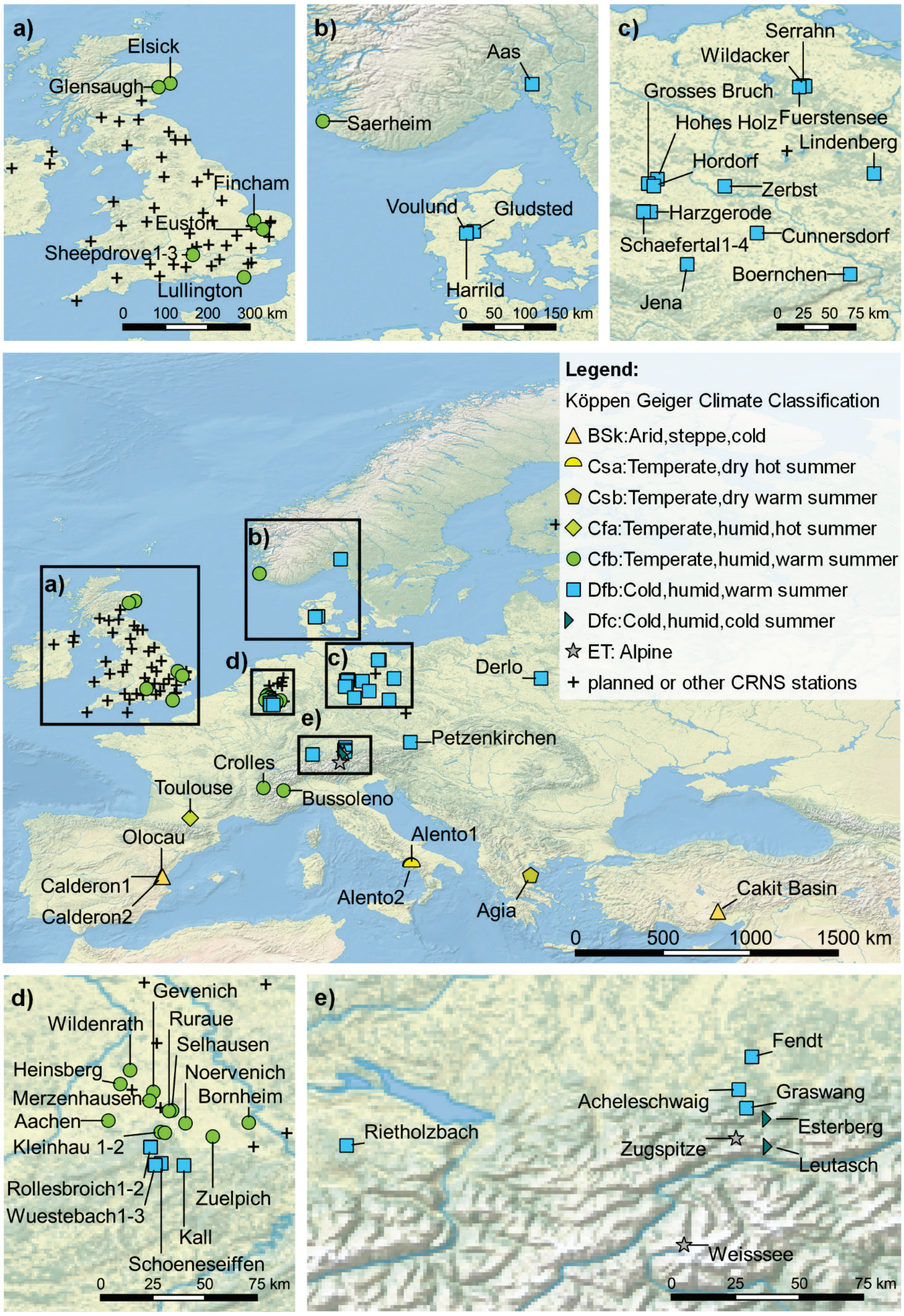

Figure 1: Locations of the COSMOS-Europe sites (the symbols show the climatic zone to which they belong) as well as sites, which are currently under construction or sites whose data we could not use.

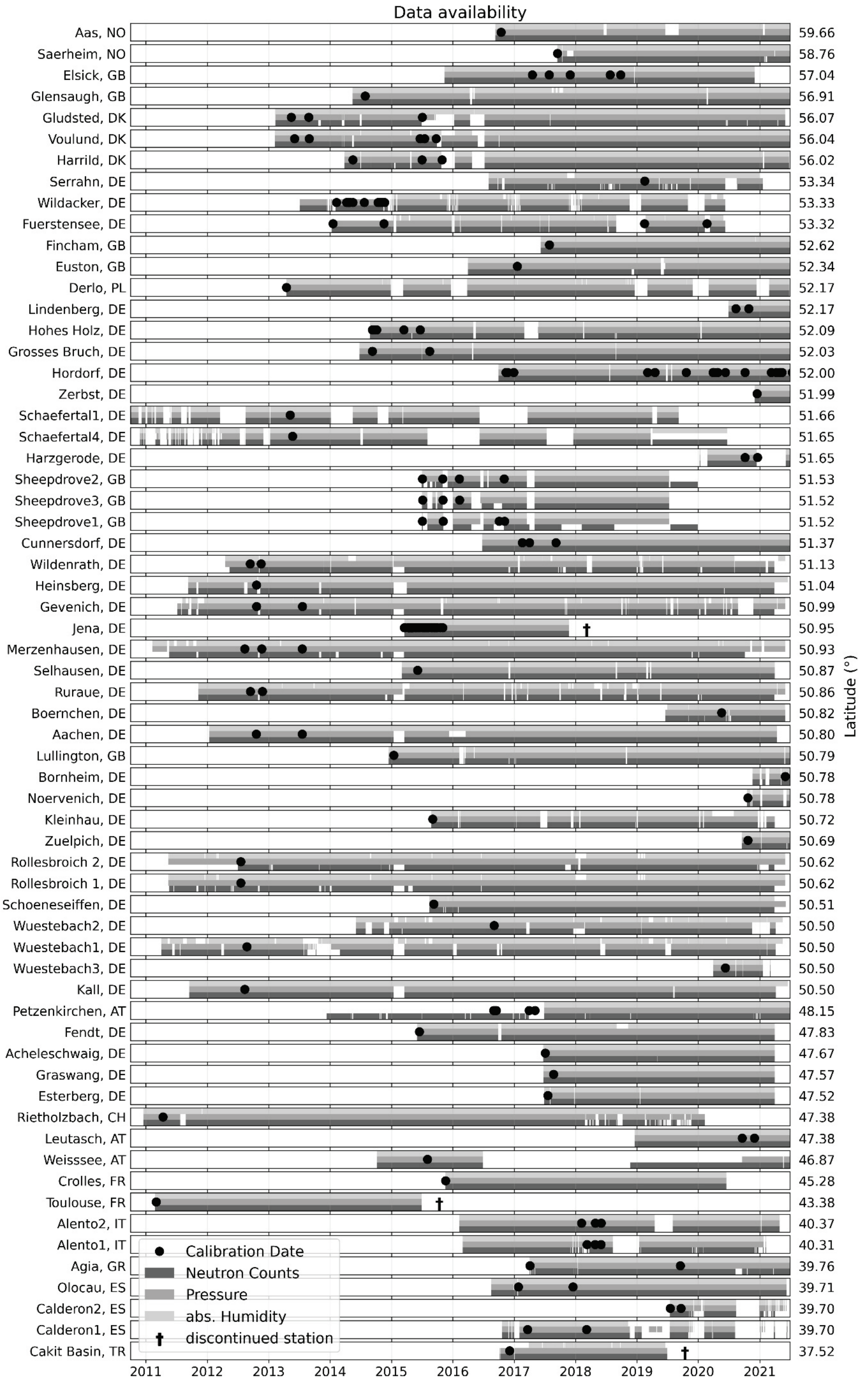
Data availability
Aas, NO 59.66
Saerheim, NO 58.76
Elsick, GB 57.04
Glensaugh, GB 56.91
Gludsted, DK 56.07
Voulund, DK 56.04
Harrild, DK 56.02
Serrahn, DE 53.34
Wildacker, DE 53.33
Fuerstensee, DE 53.32
Fincham, GB 52.62
Euston, GB 52.34
Derlo, PL 52.17
Lindenberg, DE 52.17
Hohes Holz, DE 52.09
Grosses Bruch, DE 52.03
Hordorf, DE 52.00
Zerbst, DE 51.99
Schaefertal1, DE 51.66
Schaefertal4, DE 51.65
Harzgerode, DE 51.65
Sheepdrove2, GB 51.53
Sheepdrove3, GB 51.52
Sheepdrove1, GB 51.52
Cunnersdorf, DE 51.37
Wildenrath, DE 51.13
Heinsberg, DE 51.04
Gevenich, DE 50.99
Jena, DE 50.95
Merzenhausen, DE 50.93
Selhausen, DE 50.87
Ruraue, DE 50.86
Boernchen, DE 50.82
Aachen, DE 50.80
Lullington, GB 50.79
Bornheim, DE 50.78
Noervenich, DE 50.78
Kleinhau, DE 50.72
Zuelpich, DE 50.69
Rollesbroich 2, DE 50.62
Rollesbroich 1, DE 50.62
Schoeneseiffen, DE 50.51
Wuestebach2, DE 50.50
Wuestebach1, DE 50.50
Wuestebach3, DE 50.50
Kall, DE 50.50
Petzenkirchen, AT 48.15
Fendt, DE 47.83
Acheleschwaig, DE 47.67
Graswang, DE 47.57
Esterberg, DE 47.52
Rietholzbach, CH 47.38
Leutasch, AT 47.38
Weisssee, AT 46.87
Crolles, FR 45.28
Toulouse, FR 43.38
Alento2, IT 40.37
Alento1, IT 40.31
Agia, GR 39.76
Olocau, ES 39.71
Calderon2, ES 39.70
Calderon1, ES 39.70
Cakit Basin, TR 37.52
2011
2012
2013
2014
2015
2016
2017
2018
2019
2020
2021
Latitude (°)
● Calibration Date
Neutron Counts
Pressure
abs. Humidity
† discontinued station
†
†
†

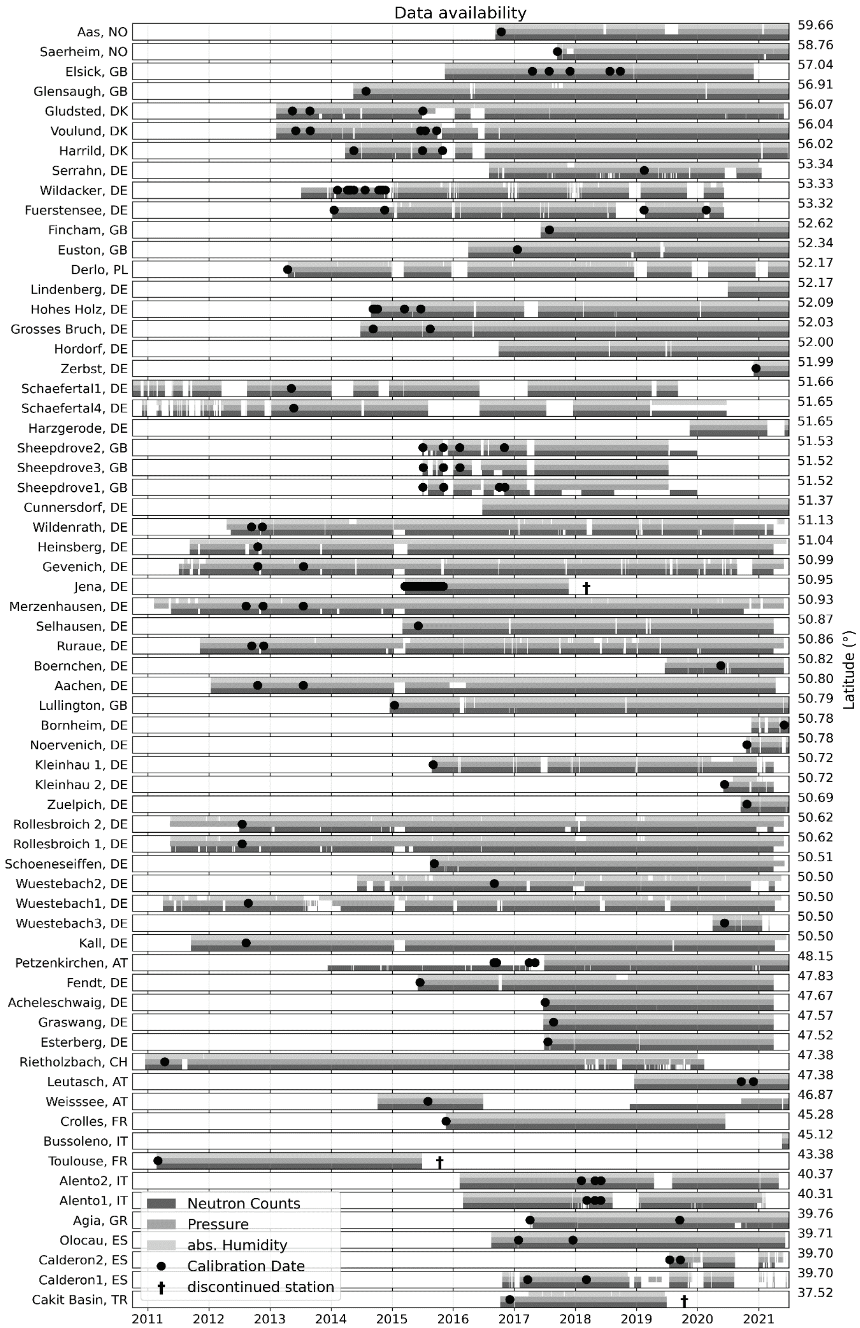

Figure 2: Availability of atmospheric pressure, absolute humidity, and neutron count rates at the COSMOS-Europe sites (sorted by descending latitude). The dates of the local reference soil sampling for CRNS calibration are also shown. The timeline shown ends in June 2021, while data and calibration dates for some sensors extend to November 2021.

Formatiert: Zeilenabstand: Mehrere 1,15 ze

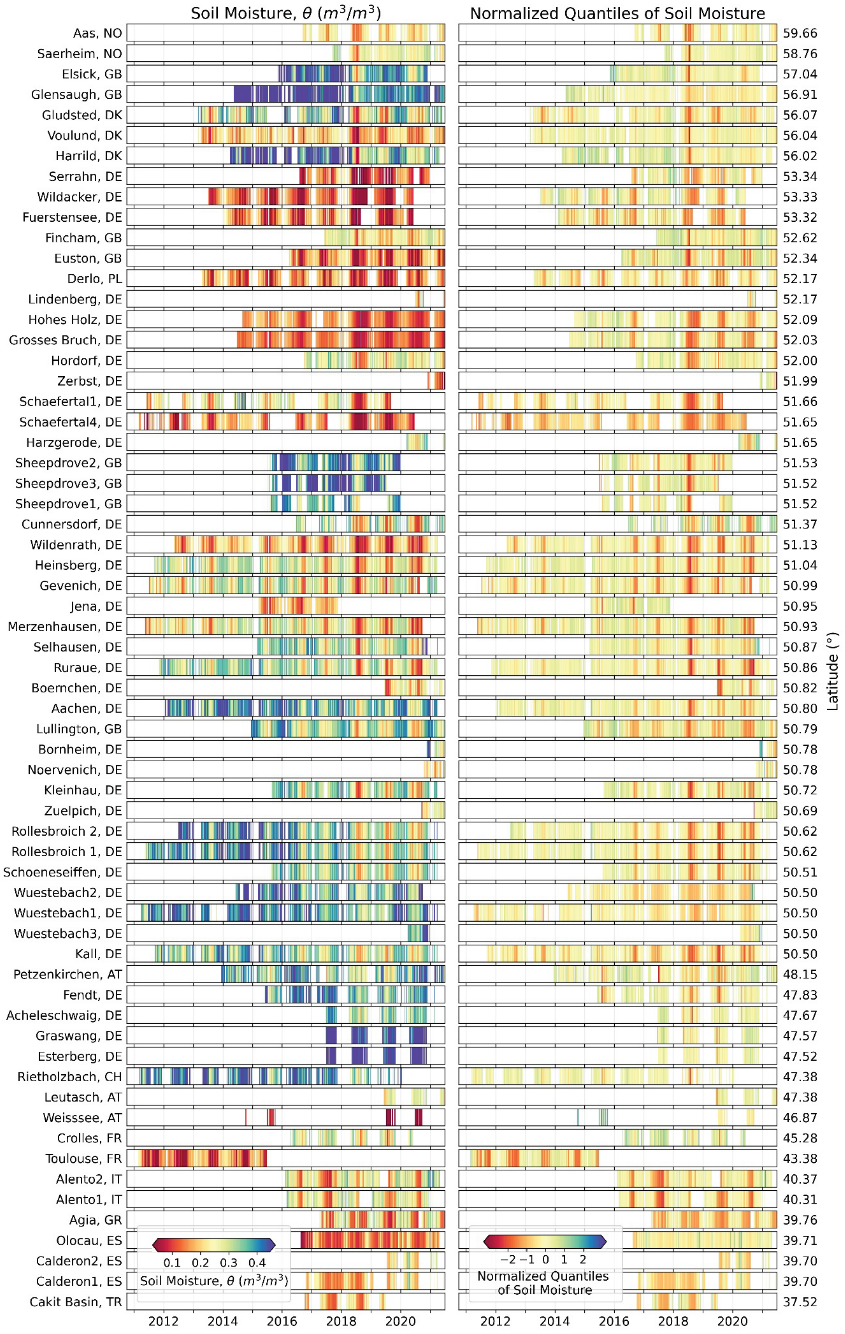
Soil Moisture, θ (m³/m³)
Normalized Quantiles of Soil Moisture
Aas, NO
Saerheim, NO
Elsick, GB
Glensaugh, GB
Gludsted, DK
Voulund, DK
Harrild, DK
Serrahn, DE
Wildacker, DE
Fuerstensee, DE
Fincham, GB
Euston, GB
Derlo, PL
Lindenberg, DE
Hohes Holz, DE
Grosses Bruch, DE
Hordorf, DE
Zerbst, DE
Schaefertal1, DE
Schaefertal4, DE
Harzgerode, DE
Sheepdrove2, GB
Sheepdrove3, GB
Sheepdrove1, GB
Cunnersdorf, DE
Wildenrath, DE
Heinsberg, DE
Gevenich, DE
Jena, DE
Merzenhausen, DE
Selhausen, DE
Ruraue, DE
Boernchen, DE
Aachen, DE
Lullington, GB
Bornheim, DE
Noervenich, DE
Kleinhau, DE
Zuelpich, DE
Rollesbroich 2, DE
Rollesbroich 1, DE
Schoeneseiffen, DE
Wuestebach2, DE
Wuestebach1, DE
Wuestebach3, DE
Kall, DE
Petzenkirchen, AT
Fendt, DE
Acheleschwaig, DE
Graswang, DE
Esterberg, DE
Rietholzbach, CH
Leutasch, AT
Weisssee, AT
Crolles, FR
Toulouse, FR
Alento2, IT
Alento1, IT
Agia, GR
Olocau, ES
Calderon2, ES
Calderon1, ES
Cakit Basin, TR
59.66
58.76
57.04
56.91
56.07
56.04
56.02
53.34
53.33
53.32
52.62
52.34
52.17
52.17
52.09
52.03
52.00
51.99
51.66
51.65
51.65
51.53
51.52
51.52
51.37
51.13
51.04
50.99
50.95
50.93
50.87
50.86
50.82
50.80
50.79
50.78
50.78
50.72
50.69
50.62
50.62
50.51
50.50
50.50
50.50
50.50
48.15
47.83
47.67
47.57
47.52
47.38
47.38
46.87
45.28
43.38
40.37
40.31
39.76
39.71
39.70
39.70
37.52
Latitude (°)
0.1 0.2 0.3 0.4
Soil Moisture, θ (m³/m³)
−2 −1 0 1 2
Normalized Quantiles of Soil Moisture
2012
2014
2016
2018
2020
2012
2014
2016
2018
2020

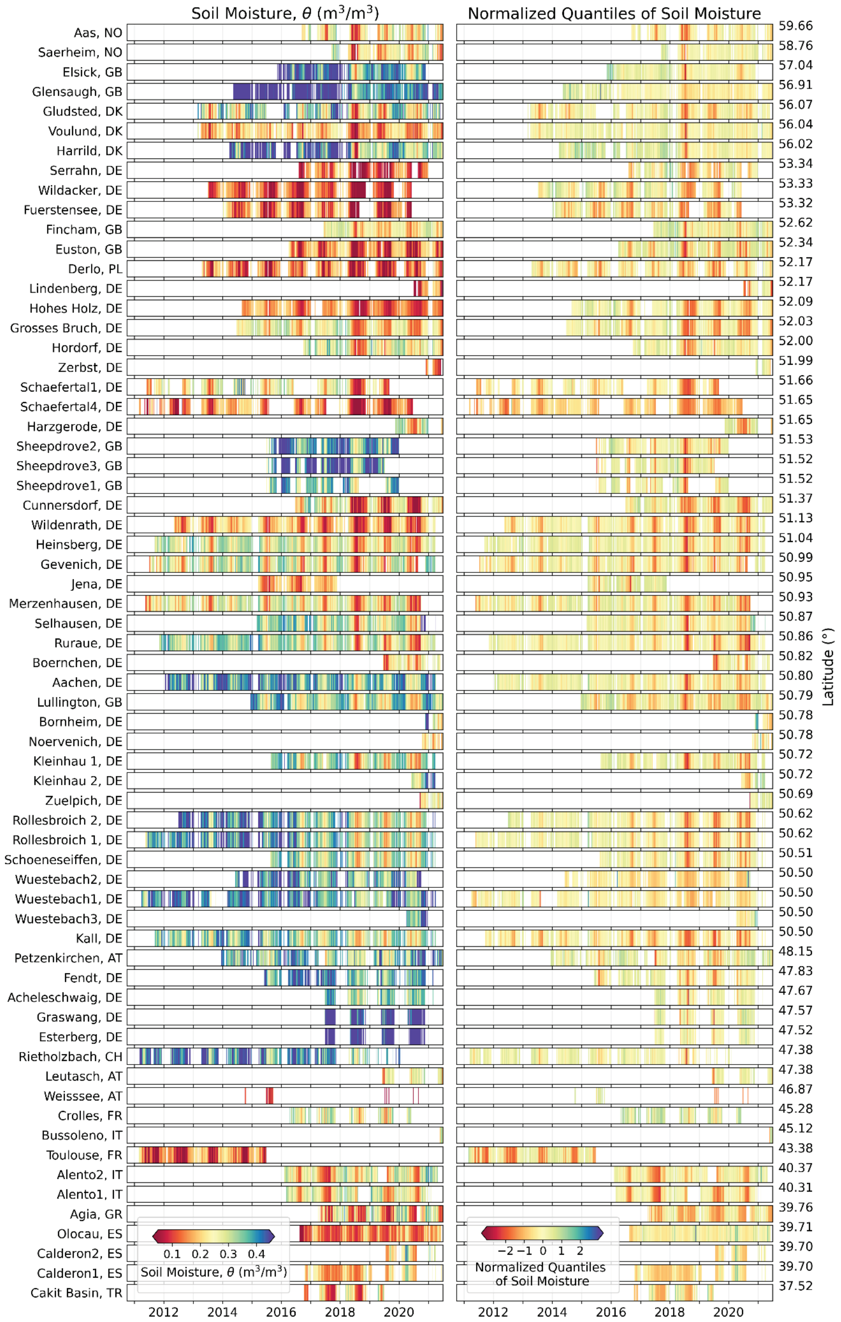

Figure 3: Time series of CRNS soil moisture (left plot) and normalized quantiles of CRNS soil moisture (right plot) of the COSMOS Europe sites ordered from north to south according to latitude (unrealistic soil moisture values are excluded, i.e., larger than porosity). The timeline shown ends in June 2021, while data and calibration dates for some sensors extend to November 2021.

Formatiert: Zeilenabstand: Mehrere 1,15 ze

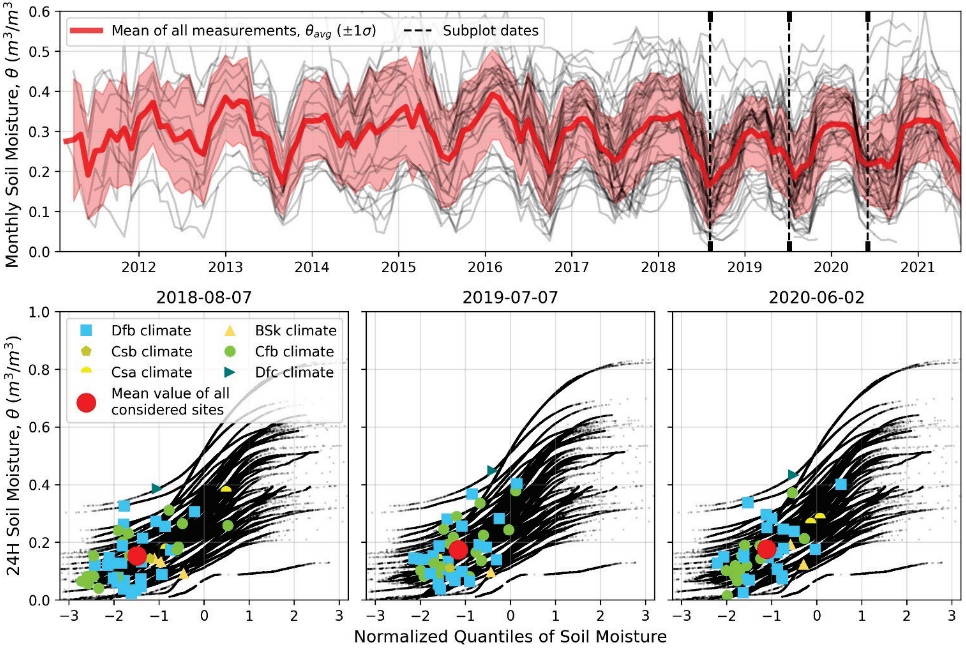

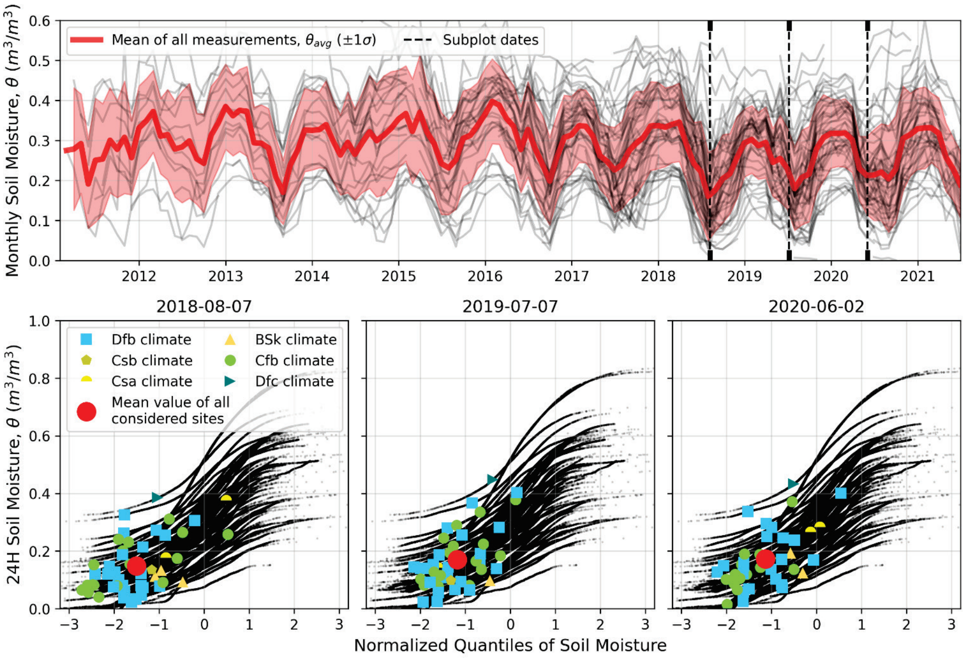

Figure 4: Time series of monthly mean CRNS soil moisture (grey lines in the upper panel) and normalized quantiles of CRNS soil moisture of the COSMOS Europe sites (black dots in the lower panels). For three exemplary days during

recent drought periods in Europe (8 August 2018, 7 July 2019 and 2 June 2020) the normalized quantiles are highlighted and differentiated by climate zone. These days were selected as they exhibited the lowest hourly soil moisture during the drought events. The mean of normalized quantiles of CRNS soil moisture for these days is also shown.

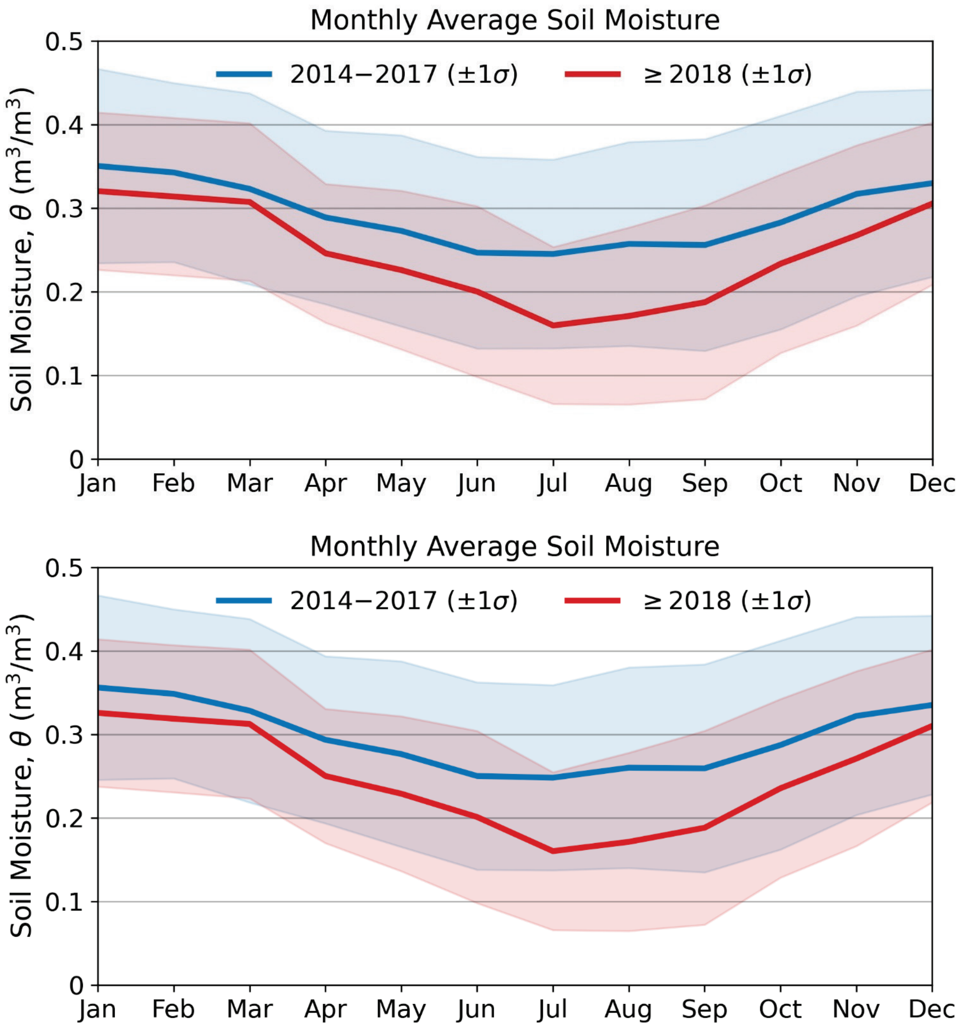

Figure 5: Comparison of monthly mean soil moisture from 2014 to 2017 and monthly mean soil moisture from 2018 to 2021 using 26 COSMOS-Europe sites that cover these periods.

Appendix

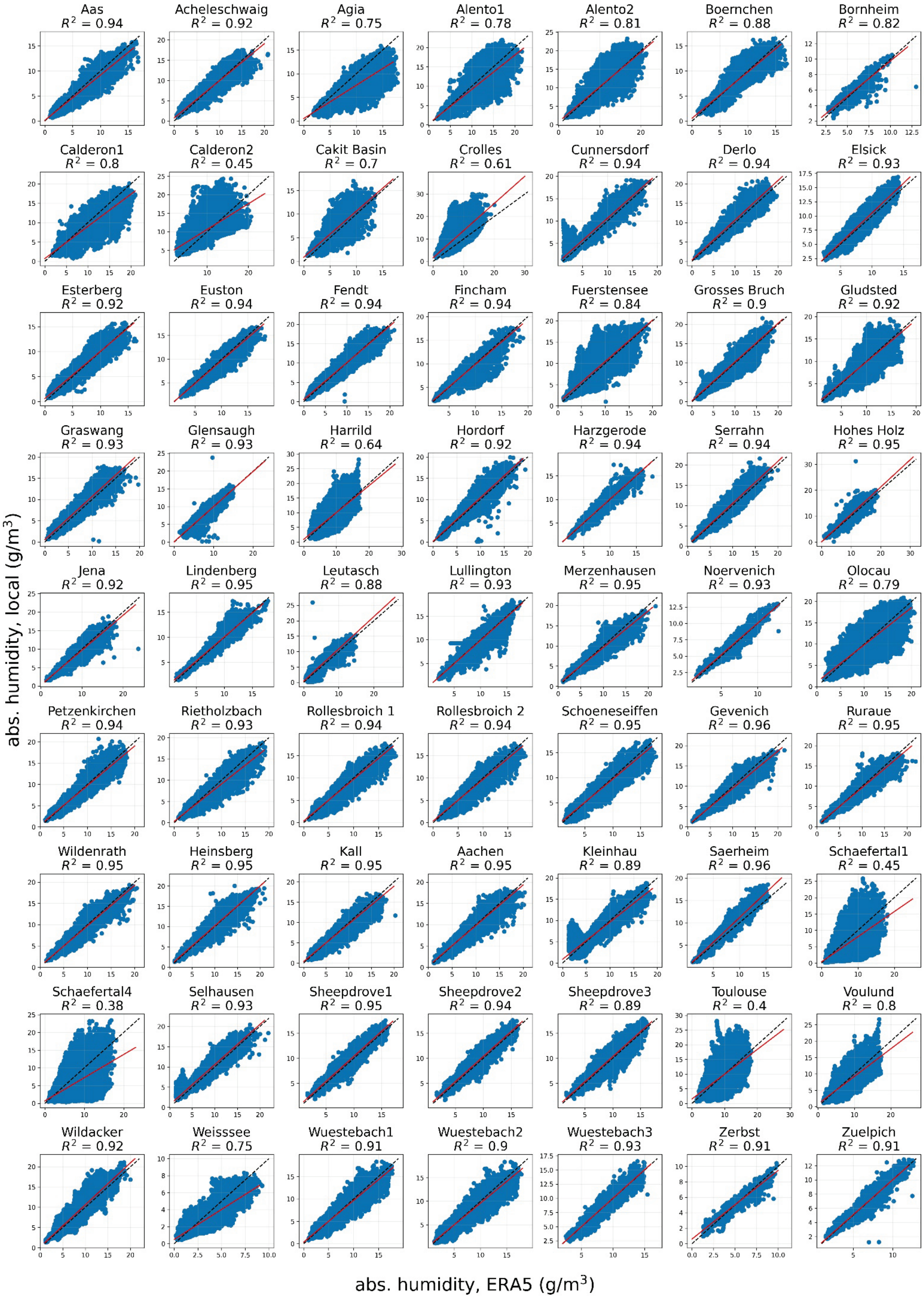
Aas R^2 = 0.94
Acheleschwaig R^2 = 0.92
Agia R^2 = 0.75
Alento1 R^2 = 0.78
Alento2 R^2 = 0.81
Boernchen R^2 = 0.88
Bornheim R^2 = 0.82
Calderon1 R^2 = 0.8
Calderon2 R^2 = 0.45
Cakit Basin R^2 = 0.7
Crolles R^2 = 0.61
Cunnersdorf R^2 = 0.94
Derlo R^2 = 0.94
Elsick R^2 = 0.93
Esterberg R^2 = 0.92
Euston R^2 = 0.94
Fendt R^2 = 0.94
Fincham R^2 = 0.94
Fuerstensee R^2 = 0.84
Grosses Bruch R^2 = 0.9
Gludsted R^2 = 0.92
Graswang R^2 = 0.93
Glensaugh R^2 = 0.93
Harrild R^2 = 0.64
Hordorf R^2 = 0.92
Harzgerode R^2 = 0.94
Serrahn R^2 = 0.94
Hohes Holz R^2 = 0.95
Jena R^2 = 0.92
Lindenberg R^2 = 0.95
Leutasch R^2 = 0.88
Lullington R^2 = 0.93
Merzenhausen R^2 = 0.95
Noervenich R^2 = 0.93
Olocau R^2 = 0.79
Petzenkirchen R^2 = 0.94
Rietholzbach R^2 = 0.93
Rollesbroich 1 R^2 = 0.94
Rollesbroich 2 R^2 = 0.94
Schoeneseiffen R^2 = 0.95
Gevenich R^2 = 0.96
Ruraue R^2 = 0.95
Wildenrath R^2 = 0.95
Heinsberg R^2 = 0.95
Kall R^2 = 0.95
Aachen R^2 = 0.95
Kleinhau R^2 = 0.89
Saerheim R^2 = 0.96
Schaefertal1 R^2 = 0.45
Schaefertal4 R^2 = 0.38
Selhausen R^2 = 0.93
Sheepdrove1 R^2 = 0.95
Sheepdrove2 R^2 = 0.94
Sheepdrove3 R^2 = 0.89
Toulouse R^2 = 0.4
Voulund R^2 = 0.8
Wildacker R^2 = 0.92
Weisssee R^2 = 0.75
Wuestebach1 R^2 = 0.91
Wuestebach2 R^2 = 0.9
Wuestebach3 R^2 = 0.93
Zerbst R^2 = 0.91
Zuelpich R^2 = 0.91
abs. humidity, local (g/m^3)
abs. humidity, ERA5 (g/m^3)

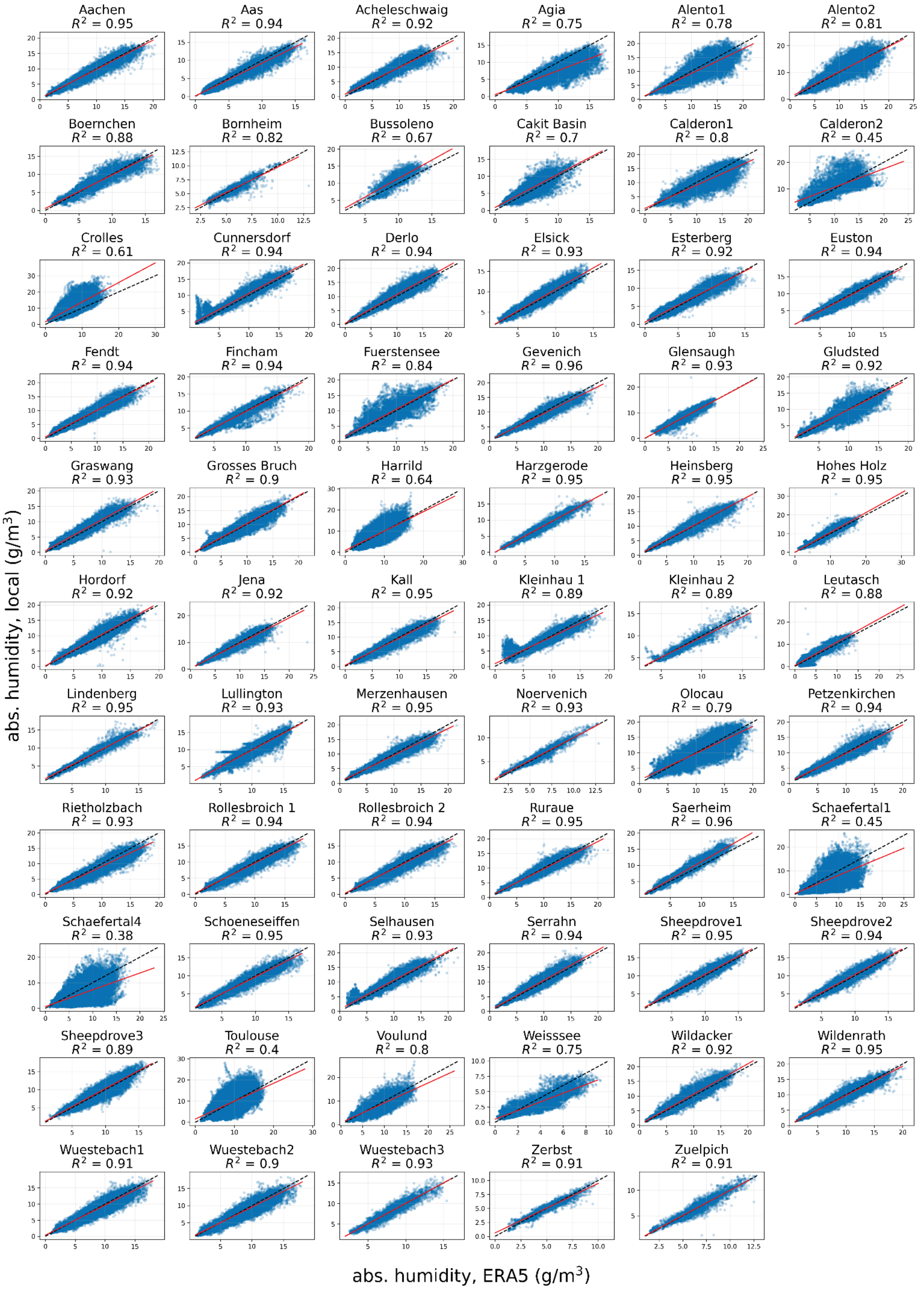

Figure A1: The correlations between air humidity from local measurements and ERA5 for the COSMOS-Europe sites.

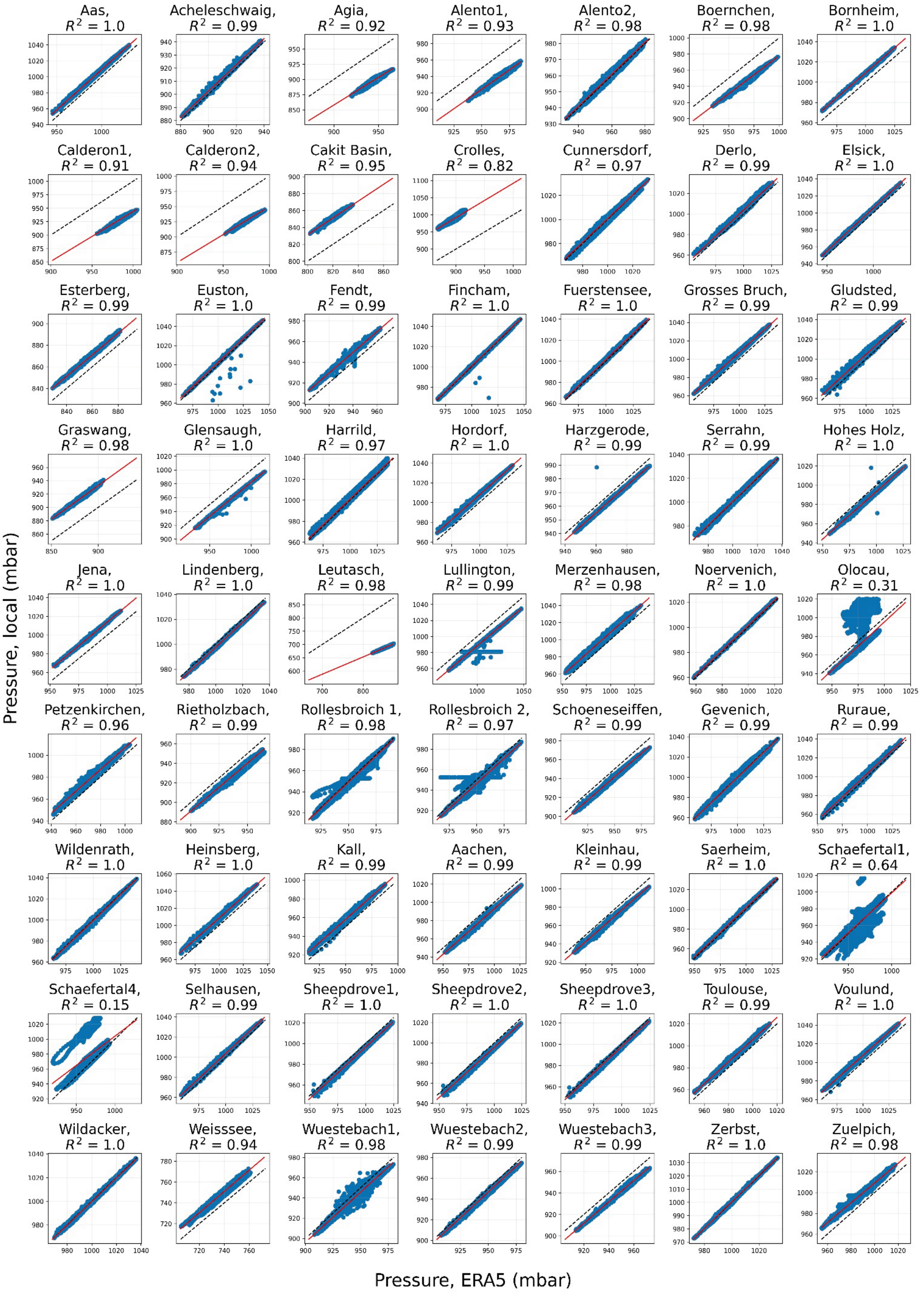
Aas, $R^2 = 1.0$
Acheleschwaig, $R^2 = 0.99$
Agia, $R^2 = 0.92$
Alento1, $R^2 = 0.93$
Alento2, $R^2 = 0.98$
Boernchen, $R^2 = 0.98$
Bornheim, $R^2 = 1.0$
Calderon1, $R^2 = 0.91$
Calderon2, $R^2 = 0.94$
Cakit Basin, $R^2 = 0.95$
Crolles, $R^2 = 0.82$
Cunnersdorf, $R^2 = 0.97$
Derlo, $R^2 = 0.99$
Elsick, $R^2 = 1.0$
Esterberg, $R^2 = 0.99$
Euston, $R^2 = 1.0$
Fendt, $R^2 = 0.99$
Fincham, $R^2 = 1.0$
Fuerstensee, $R^2 = 1.0$
Grosses Bruch, $R^2 = 0.99$
Gludsted, $R^2 = 0.99$
Graswang, $R^2 = 0.98$
Glensaugh, $R^2 = 1.0$
Harrild, $R^2 = 0.97$
Hordorf, $R^2 = 1.0$
Harzgerode, $R^2 = 0.99$
Serrahn, $R^2 = 0.99$
Hohes Holz, $R^2 = 1.0$
Jena, $R^2 = 1.0$
Lindenberg, $R^2 = 1.0$
Leutasch, $R^2 = 0.98$
Lullington, $R^2 = 0.99$
Merzenhausen, $R^2 = 0.98$
Noervenich, $R^2 = 1.0$
Olocau, $R^2 = 0.31$
Petzenkirchen, $R^2 = 0.96$
Rietholzbach, $R^2 = 0.99$
Rollesbroich 1, $R^2 = 0.98$
Rollesbroich 2, $R^2 = 0.97$
Schoeneseiffen, $R^2 = 0.99$
Gevenich, $R^2 = 0.99$
Ruraue, $R^2 = 0.99$
Wildenrath, $R^2 = 1.0$
Heinsberg, $R^2 = 1.0$
Kall, $R^2 = 0.99$
Aachen, $R^2 = 0.99$
Kleinhau, $R^2 = 0.99$
Saerheim, $R^2 = 1.0$
Schaefertal1, $R^2 = 0.64$
Schaefertal4, $R^2 = 0.15$
Selhausen, $R^2 = 0.99$
Sheepdrove1, $R^2 = 1.0$
Sheepdrove2, $R^2 = 1.0$
Sheepdrove3, $R^2 = 1.0$
Toulouse, $R^2 = 0.99$
Voulund, $R^2 = 1.0$
Wildacker, $R^2 = 1.0$
Weisssee, $R^2 = 0.94$
Wuestebach1, $R^2 = 0.98$
Wuestebach2, $R^2 = 0.99$
Wuestebach3, $R^2 = 0.99$
Zerbst, $R^2 = 1.0$
Zuelpich, $R^2 = 0.98$
Pressure, local (mbar)
Pressure, ERA5 (mbar)

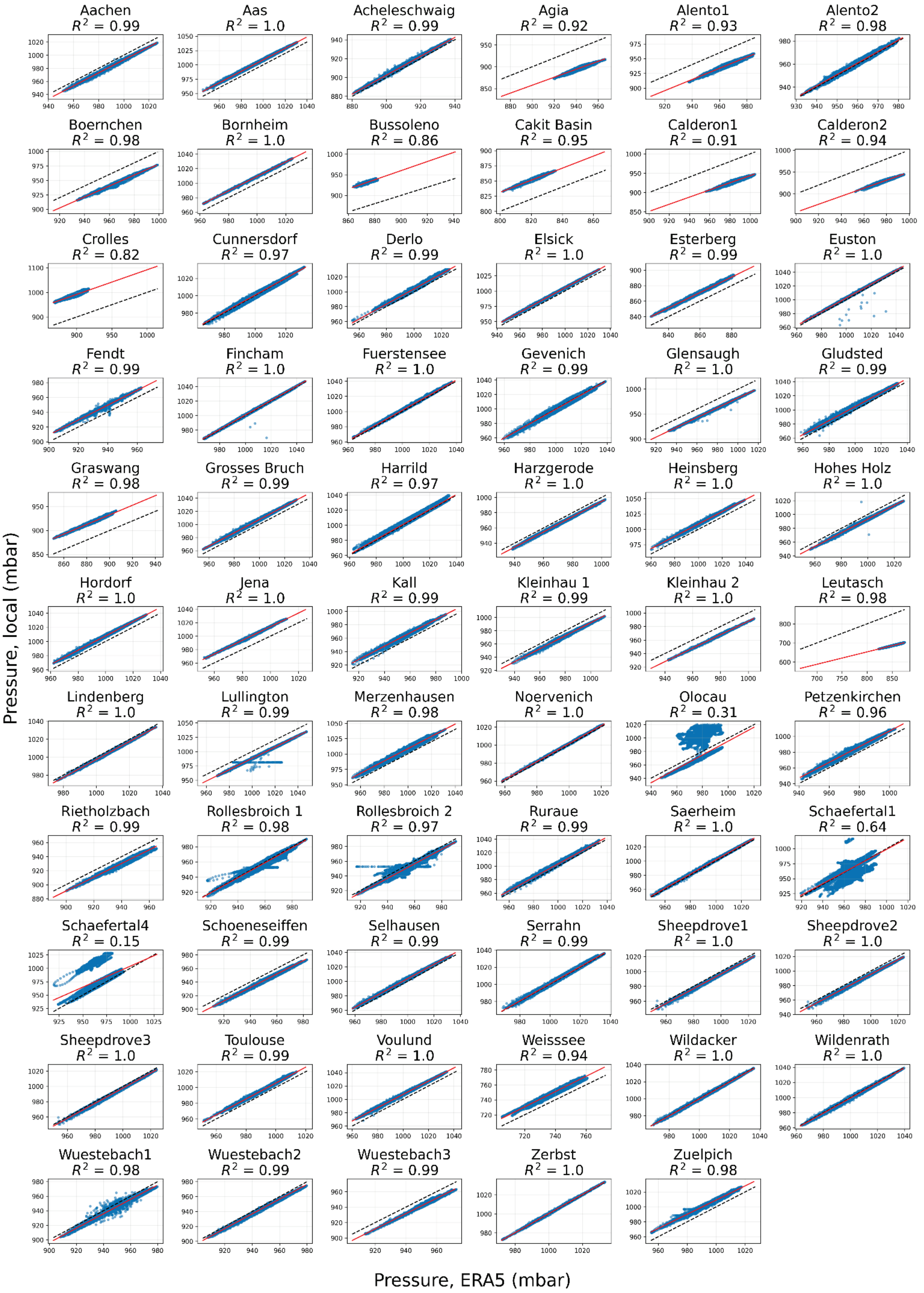

Figure A2: The correlations between atmospheric pressure from local measurements and ERA5 for the COSMOS-Europe sites.

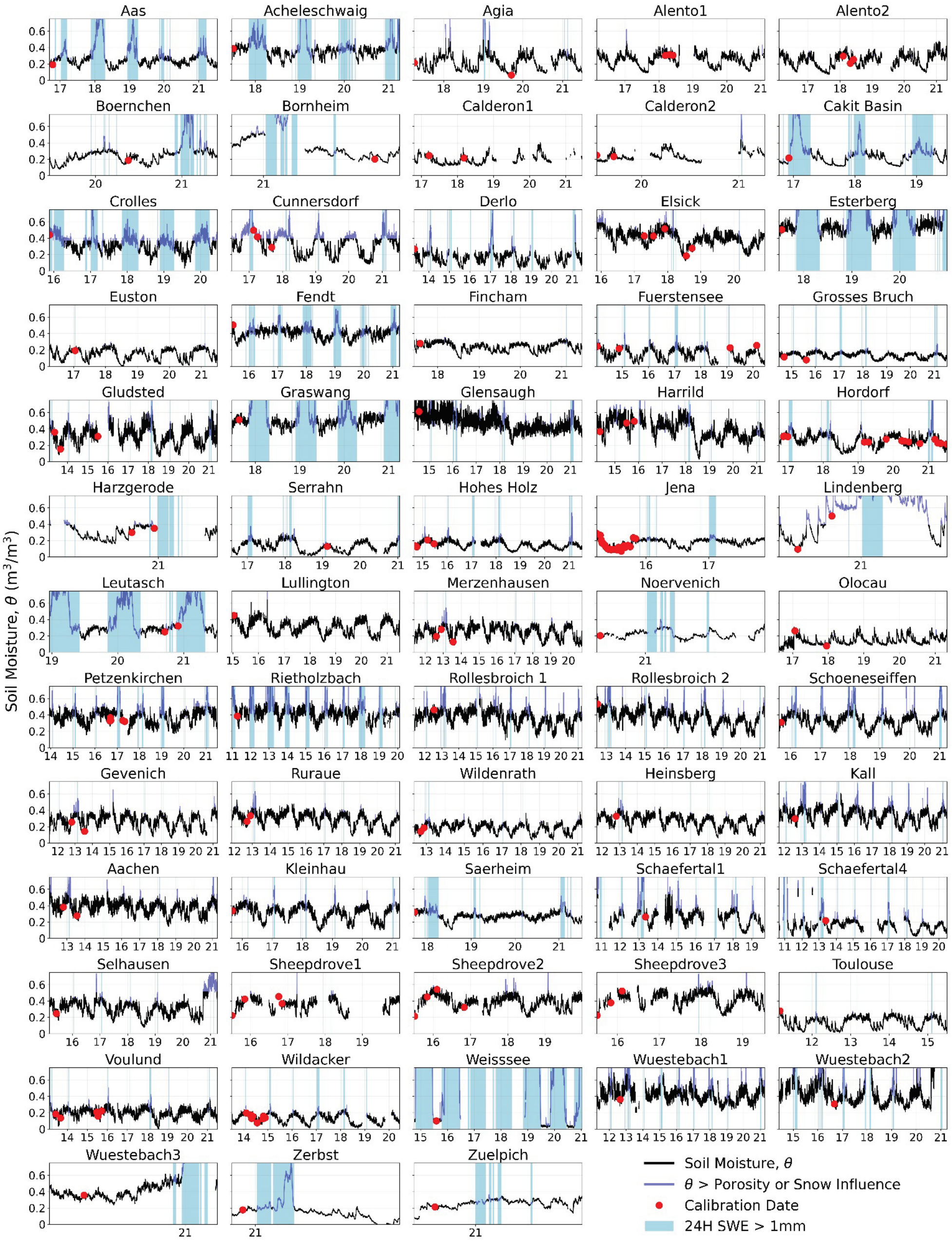
Aas
Acheleschwaig
Agia
Alento1
Alento2
Boernchen
Bornheim
Calderon1
Calderon2
Cakit Basin
Crolles
Cunnersdorf
Derlo
Elsick
Esterberg
Euston
Fendt
Fincham
Fuerstensee
Grosses Bruch
Gludsted
Graswang
Glensaugh
Harrild
Hordorf
Harzgerode
Serrahn
Hohes Holz
Jena
Lindenberg
Leutasch
Lullington
Merzenhausen
Noervenich
Olocau
Petzenkirchen
Rietholzbach
Rollesbroich 1
Rollesbroich 2
Schoeneseiffen
Gevenich
Ruraue
Wildenrath
Heinsberg
Kall
Aachen
Kleinhau
Saerheim
Schaefertal1
Schaefertal4
Selhausen
Sheepdrove1
Sheepdrove2
Sheepdrove3
Toulouse
Voulund
Wildacker
Weisssee
Wuestebach1
Wuestebach2
Wuestebach3
Zerbst
Zuelpich
Soil Moisture, θ (m³/m³)
0
0.2
0.4
0.6
Soil Moisture, θ
θ > Porosity or Snow Influence
Calibration Date
24H SWE > 1mm

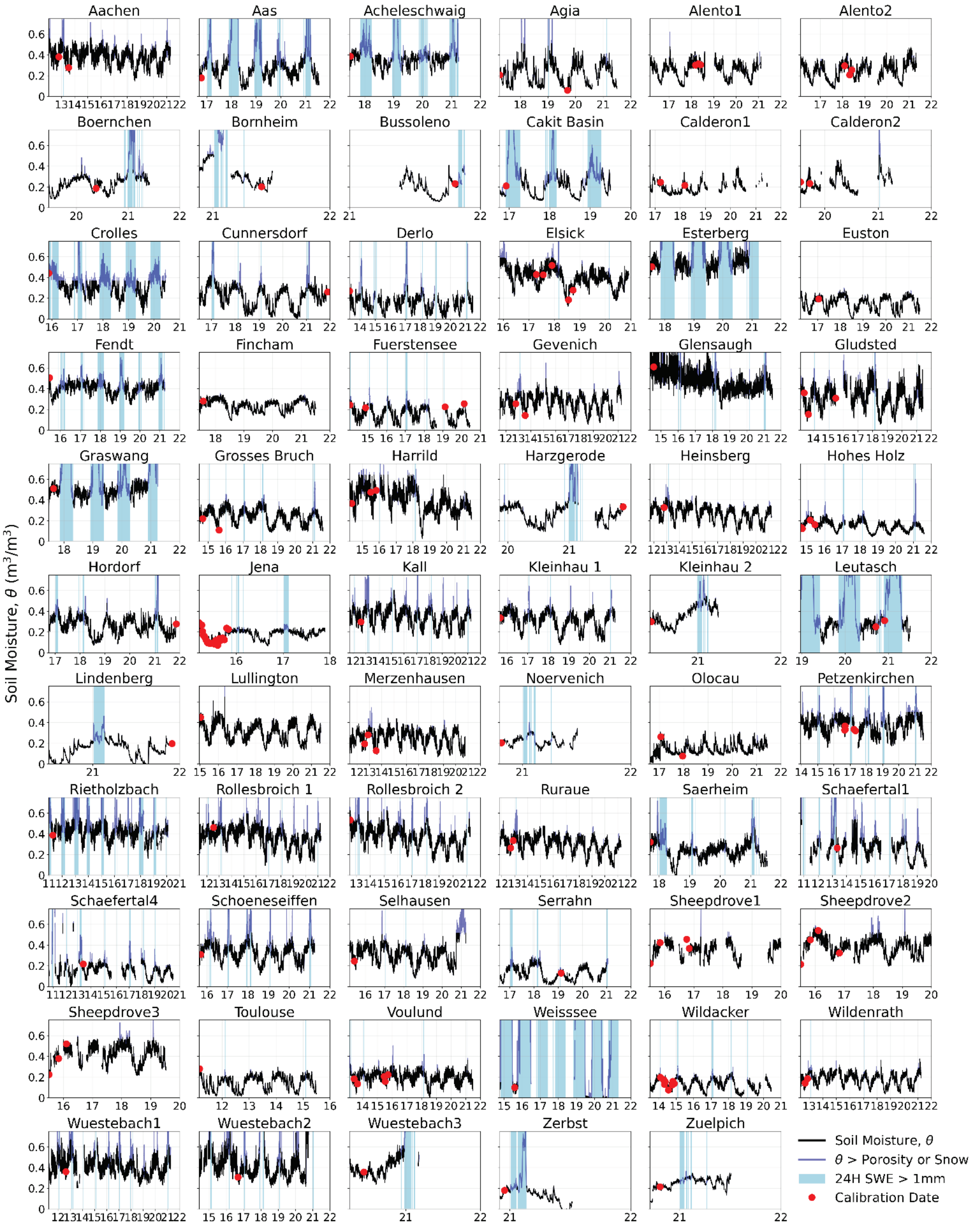

Figure A3: Detected unrealistic CRNS soil moisture estimates due the presence of snow at the site (i.e. times of snow water equivalent from ERA5 larger than 1 mm) and soil moisture values exceeding the local soil porosity.

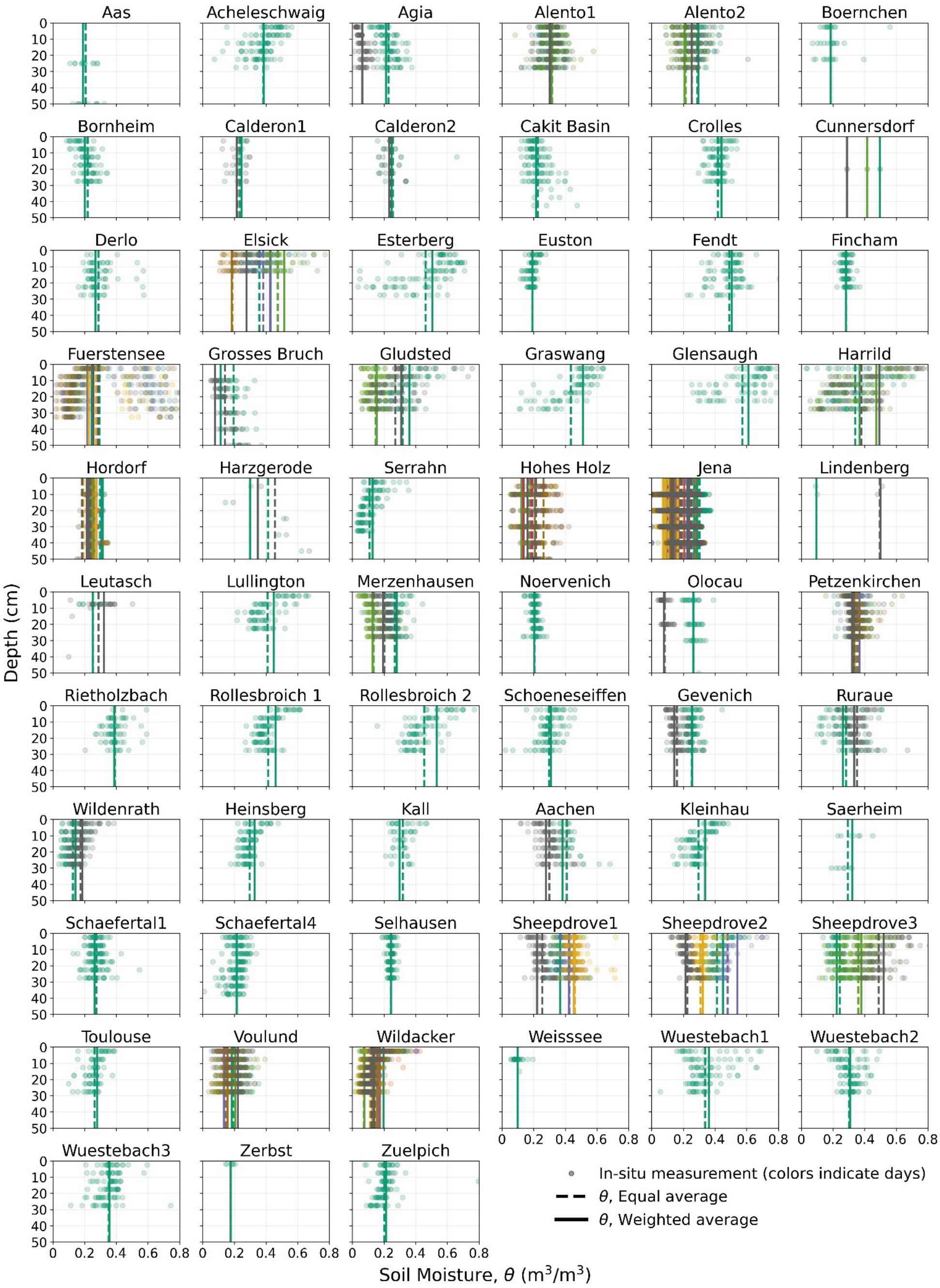
Aas
Acheleschwaig
Agia
Alento1
Alento2
Boernchen
Bornheim
Calderon1
Calderon2
Cakit Basin
Crolles
Cunnersdorf
Derlo
Elsick
Esterberg
Euston
Fendt
Fincham
Fuerstensee
Grosses Bruch
Gludsted
Graswang
Glensaugh
Harrild
Hordorf
Harzgerode
Serrahn
Hohes Holz
Jena
Lindenberg
Leutasch
Lullington
Merzenhausen
Noervenich
Olocau
Petzenkirchen
Rietholzbach
Rollesbroich 1
Rollesbroich 2
Schoeneseiffen
Gevenich
Ruraue
Wildenrath
Heinsberg
Kall
Aachen
Kleinhau
Saerheim
Schaefertal1
Schaefertal4
Selhausen
Sheepdrove1
Sheepdrove2
Sheepdrove3
Toulouse
Voulund
Wildacker
Weisssee
Wuestebach1
Wuestebach2
Wuestebach3
Zerbst
Zuelpich
Depth (cm)
0
10
20
30
40
50
0
0.2
0.4
0.6
0.8
Soil Moisture, θ (m^3/m^3)
In-situ measurement (colors indicate days)
θ, Equal average
θ, Weighted average

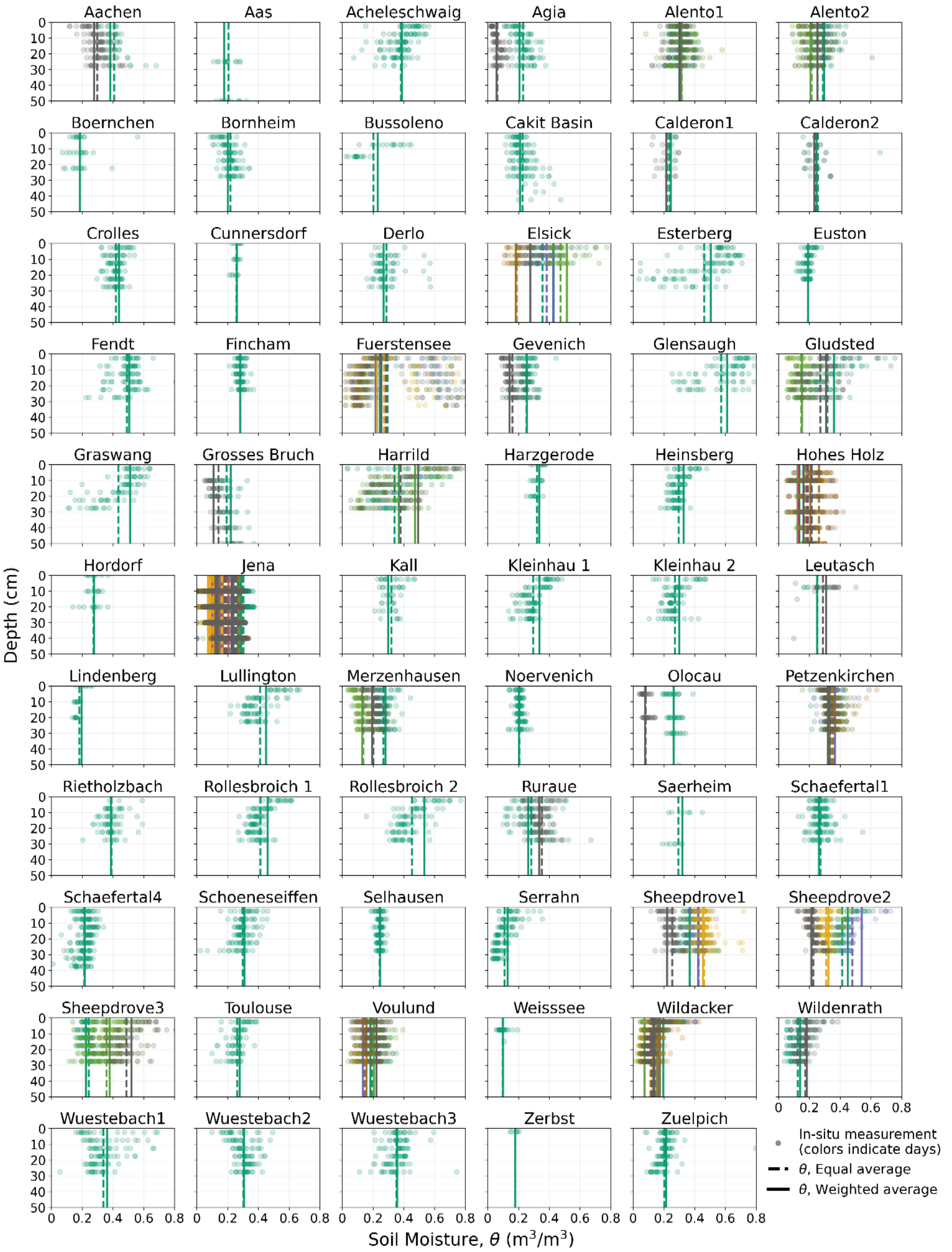

Figure A4: Soil profiles of the in-situ calibration data for the COSMOS-Europe sites. The weighted average soil moisture values are also shown. The varying colours indicate the different sampling dates.

(a) Metadata information

- Station owner/responsible and affiliation
- Geographic coordinates and altitude
- Time series range
- Station description and physical quantities according Table 2 (e.g., cutoff rigidity)
- Calibration data:
  Calibration Time, SM (g/g), BD (g/cm^3), SOC (g/g), LW (g/g)

(b) Raw CRNS and meteorological data

- Timestamp
- NeutronCount_Epithermal_Cum1hr
- NeutronCount_Slow_Cum1hr
- AirTemperature in (degC)
- AirHumidity_Relative in (%_Sat)
- AirPressure in (mbar)
- Precipitation_Cum1h in (mm)

Processed CRNS data and diagnostics

- AirHumidity_absolute_Avg1h
- NeutronCount_Epithermal_Cum1h_corrected
- NeutronCount_Epithermal_Cum1h_corrected_std
- NeutronCount_Epithermal_MovAvg24h_corrected
- NeutronCount_Epithermal_MovAvg24h_corrected_std
- SoilMoisture_volumetric_MovAvg24h
- SoilMoisture_volumetric_MovAvg24h_std_upper
- SoilMoisture_volumetric_MovAvg24h_std_lower
- SoilMoisture_volumetric_MovAvg24h_std
- Sensor_Footprint_Radius
- Sensor_Footprint_Depth
- Flag_Outlier_NeutronCount
- Flag_Porosity_Excess
- Flag_Snow_ERA5
- Flag_AirPressure_ERA5
- Flag_AirHumidity_ERA5

(c) Calibration raw data

- Timestamp
- Profile_ID
- Distance_to_CRNS in (m)
- Profile_Depth in (m)
- SoilMoisture in (g/g)
- DryBulkDensity in (g/cm^3)
- SoilOrganicCarbon (g/g)
- LatticeWater in (g/g)

(a) Metadata information

- Station owner/responsible and affiliation
- Geographic coordinates and altitude
- Time series range
- Station description and physical quantities according Table 2 (e.g., cutoff rigidity)
- Calibration data:
  Calibration Time, SM (g/g), BD (g/cm^3), SOC (g/g), LW (g/g)

(b) Raw CRNS and meteorological data

- Timestamp
- NeutronEpithermalCount_Cum1hr
- NeutronSlowCount_Cum1hr
- AirTemperature in (degC)
- AirHumidity_Relative in (%_Sat)
- AirPressure in (mbar)
- Precipitation in (mm)

Processed CRNS data and diagnostics

- AirHumidity_Flag_ERA5
- AirPressure_Flag_ERA5
- Footprint_Depth_Avg1hr in (m)
- Footprint_Radius_Avg1hr in (m)
- NeutronCount_OutlierFlag
- NeutronEpithermalCount_Cum1hr_Corr
- NeutronEpithermalCount_Sdev1hr_Corr
- NeutronEpithermalCount_MovAvg24h_Cum1hr_Corr
- NeutronEpithermalCount_MovAvg24h_Sdev1hr_Corr
- SnowWaterEquivalent_Flag_ERA5
- SoilWaterContent_PorosityExcess
- SoilWaterContent_MovAvg24h
- SoilWaterContent_Sdevu24h
- SoilWaterContent_Sdevu24h
- SoilWaterContent_Sdev24h

(c) Calibration raw data

- Timestamp
- SampleCount
- SensorDistance in (m)
- SCSmpLevel in (m)
- SoilWaterContent in (g/g)
- SoilBulkDensity in (g/cm^3)
- SoilConcentrationTOC in (g/g)
- SoilLatticeWaterContent in (g/g)

Figure A5: Data structure in the TERENO Data Discovery Portal (DDP). Each station comprises metadata (a) with detailed site information and two time series. One time series contains the raw CRNS data, the meteorological data and the processed data with the associated diagnostics (b). The second time series provides the raw calibration data (c).